USING GROUND-BASED LIDAR TO ANALYZE FRACTURE CHARACTERISTICS AS POSSIBLE CONTROLS ON THE VARIABILITY OF VALLEY MORPHOLOGY IN THE BUFFALO RIVER WATERSHED, ARKANSAS

By

Jamison N. Braun

A thesis submitted to the Graduate Faculty of
Auburn University
in partial fulfillment of the
requirements for the Master of Science
Degree in Geology

Auburn, Alabama
August 7th, 2021

Keywords: LiDAR, valley morphology, erosion, fractures, lithologic strength

Approved by

Dr. Stephanie Shepherd, Chair, Assistant Professor of Geoscience
Dr. Lorraine Wolf, Professor of Geology
Dr. Ashraf Uddin, Professor of Geology

Abstract

The Buffalo National River (BNR) is a bedrock river that incises a sequence of Ordovician and Mississippian sedimentary rocks as it meanders west to east across the southern point of the Ozark Dome. A previous study utilizing a Geographic Information System (GIS) has found that there are four main lithologic reaches of the BNR. Two reaches are composed mainly of the Mississippian Boone Formation, which is made up of limestone with prominent chert beds, and two reaches are composed mainly of the Ordovician Everton Formation, which is made up of mostly quartz arenite. Boone Formation reaches have been found to have a larger valley width than Everton Formation reaches. Previous studies have shown that the variability in valley width can be attributed to the differential chemical weathering of these two formations, but to date the variability of fracture characteristics within each formation have not been studied. Spacing and orientation of fractures in rocks exert strong controls on river morphology at the reach and outcrop scale. Using a combination of terrestrial LiDAR scans and field techniques, the fracture characteristics of each of these formations have been analyzed. These data were then synthesized into a common geomechanical classification scheme. Data from the field indicate that the variability in valley width of the BNR can be attributed to the highly brecciated nature of the chert beds of the Boone Formation. An understanding of the distribution of fractures within formations is essential to determining a mechanistic understanding of the morphology of bedrock rivers as a whole. Across landscapes, fractures focus erosion resulting in incision that follows fracture patterns. If rock erodibility is assumed to scale with fracture density, then an analysis of fracture characteristics on the Boone and Everton formations determines a potential first-order control on the development of valley morphology within the BNR.

Acknowledgements

Partial funding for this thesis was provided through a National Science Foundation grant (NSF-EAR- 324869 - Geomorphology and Land Use Dynamics Program). Travel funding for this research was provided by the Geoscience Advisory Board at Auburn University. I would like to thank the following people at Auburn University who devoted their time and gave helpful advice in the completion of this thesis: Dr Shepherd, Dr. Wolf, Dr. Uddin, and the whole of the faculty at Auburn. I would also like to give a special thanks to Dr. Shepherd, as she was available for help with any topic whenever I needed it. A special thanks to Brian Norton of Split Engineering, as his help navigating the Split-FX program was immensely appreciated. Richard Hutto, of the Arkansas Geological Survey, was invaluable during my time spent in the field. His regional expertise aided in scouting locations, and his cheerful disposition helped keep morale high during the heavy rain we experienced in the field. Lastly, I would like to thank my family and friends for providing constant, unwavering support throughout this process.

Table of Contents

List of Tables

List of Figures

List of Abbreviations

BNR	Buffalo National River
BNRW	Buffalo National River Watershed
DD	Dip Direction
GIS	Geographic Information System
ISRM	International Society for Rock Mechanics
LiDAR	Light Detection and Ranging
MUD	Multiples of Uniform Density
RMR	Rock Mass Rating System
RMR_B	Basic Rock Mass Rating System
RMS	Rock Mass Strength
RQD	Rock Quality Designation
SH	Schmidt Hammer
UCS	Uniaxial Compressive Strength

Chapter 1: Thesis Introduction

Introduction

The Buffalo National River Watershed (BNRW) in Northern Arkansas has been shown by (Keen-Zebert et al., 2017) to have atypical valley form. Rivers tend to form valleys that are narrow at their headwaters and become wider moving downstream. In contrast, the Buffalo National River (BNR) alternates between narrow and wide valleys as it flows from west to east through the Ozark Dome (Heidner, 2019). As it meanders, the BNR incises into three major physiographic provinces. These provinces are the Springfield Plateau, Salem Plateau, and Boston Mountains, with the majority of the BNR incising the Springfield Plateau and Boston Mountains (Fig. 1) (Kuniansky, 2011). As it cuts through the plateau surfaces, the BNR exposes the Ordovician Everton Formation, which is composed predominantly of quartz arenites (Hudson and Murray, 2003). It also exposes the Mississippian Boone Formation, which is composed largely of various carbonate rocks (Braden et al., 2003). Current research suggests that differential weathering of the Boone and Everton Formations is the primary control on valley morphology of the BNR (Keen-Zebert et al., 2017; Heidner, 2019). Chemical weathering has been found to exert a higher control on the development of valley morphology than mechanical weathering processes. The Boone and Everton Formations have low variability in the mechanical resistances of rock types within each formation. Work by Keen-Zebert et al. (2017) has shown that in reaches composed predominantly of the more resistant Everton Formation, valley width is narrower than that of reaches composed dominantly of the Boone Formation.

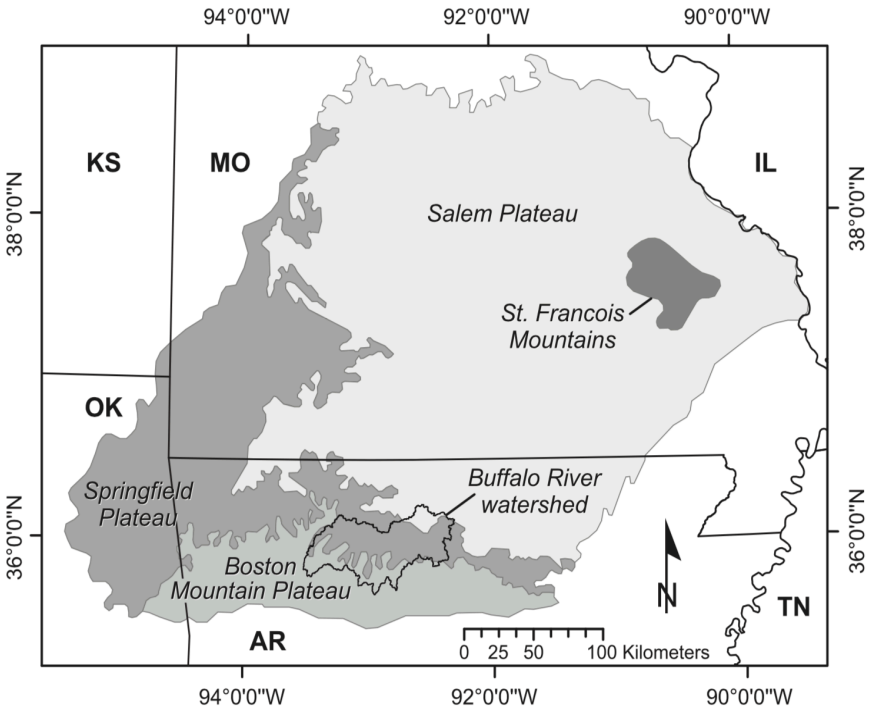

Figure 1: Map of the Ozark physiographic province. The study area is inside the area labeled as "Buffalo River Watershed". The Buffalo River flows from west to east while mainly incising the Springfield Plateau; from Keen-Zebert et al. (2017).

An influential study of the Henry Mountains in Colorado by G.K. Gilbert (1877) documented various controls on valley form. In this study he analyzed the role of lithology in the development of valley form, noting that in more resistant sandstone beds the river valley was narrower than in less resistant shale beds. Gilbert (1877) concluded that when downward erosion slows, lateral abrasion exerts a greater control on the valley form. Like the Henry Mountains, the BNR incises through sedimentary layers that exhibit differential erosional resistance. Previous studies in the BNR have focused on measuring mechanical and chemical erosional resistance of the two major units, the Boone and Everton formations, exposed at river level (Keen-Zebert et al. 2017; Heidner, 2019). Research by Keen-Zebert et al. (2017) and Heidner (2019) in the BNR does not refute Gilbert's conclusion but suggests the role of lithology is much more complex than he originally thought. While it is clear lithology is of importance to valley form, it is unclear

how the fracture characteristics of the variable lithologies exposed along the BNR influence erosional processes.

Objectives

The objective of this study is to investigate the spacing, density, orientation, and size of fractures and other discontinuities present at Roark Bluff and White Bluff, two cliff faces along meander bends in the BNR that contain exposures of the Everton and Boone formations, respectively. In addition, a comprehensive geomechanical classification of the Boone and Everton Formations derived from scanline measurements at various locations along the BNR are used to draw conclusions about the stability of these formations. Combining remote sensing and field-based methods will serve to answer the following question: How do fractures within the Boone and Everton formations influence the erosional processes that shape the valley morphology of the BNR?

Previous Research

The study by Keen-Zebert et al. (2017) focused on determining the effect of lithology on valley width, terrace distribution, and bedload provenance within the Buffalo River Watershed. Keen-Zebert et al. (2017) defined four reaches within the Buffalo River Watershed based on the primary lithology exposed at river level (Figure 2). Measurements of mechanical and chemical resistance were collected within each reach. Mechanical resistance measurements were conducted in the field using a Schmidt Hammer, and measurements of chemical resistance were conducted in the laboratory. A decarbonation method was used to estimate the percent solubility of various lithologies within the catchment (Keen-Zebert et al., 2017).

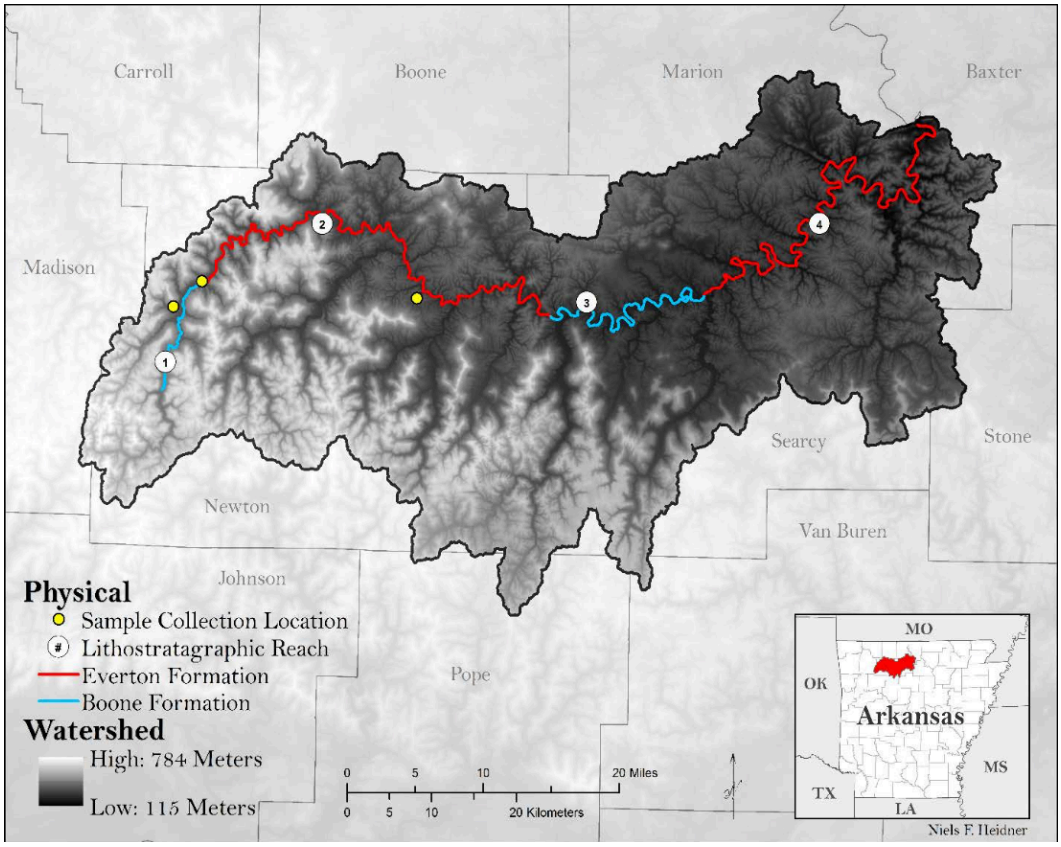

Figure 2: Map of the BNRW with reach numbers displayed, as well as blue and red highlights along the river where it incises the Boone and Everton formations; From Heidner (2019).

The Everton and Boone Formations were found to have similar mechanical resistance, but the Everton Formation is more chemically resistant than the Boone Formation. The Everton Formation reaches have smaller valley width than the Boone Formation on average, and this has been attributed to the higher chemical resistance of the Everton Formation (Keen-Zebert et al., 2017).

The most recent research conducted within the Buffalo River Watershed is the thesis work of Niels Heidner (2019). This research utilized experimental techniques – abrasion mills to test the mechanical weathering potential and dissolution experiments to quantify chemical weathering potential – to further our understanding of differential erosion in the Boone and

Everton formations. In summary, this work confirmed previous findings that erodibility varies between the formations of the BNRW and varies within each formation (Heidner, 2019).

Chapter 2: Literature Review

Effects of Lithology on Rock Strength

In his seminal study of the geology of the Henry Mountains, G. K. Gilbert (1877) discussed erosional processes that fundamentally changed how many geomorphologists study landforms and landscape change. He proposed that there are three main conditions that affect the speed at which rock erodes. These are declivity, character of the rock, and climate. The "character of the rock" in this context simply means the strength of the rock that is being eroded. Empirically, Gilbert (1877) found that hard rocks have a higher resistance to erosional forces than soft rocks, and his work focused largely on a qualitative approach to studying how rock strength influences the development of landscapes. Contemporaries of Gilbert took a qualitative approach as well, with John Wesley Powell writing of the Colorado River in 1895: "Along its course where the rocks are hard, the stream is narrow and swift, with rapids and falls; where the rocks are soft, it is wide and quiet" (Bursztyn et al., 2015).

It was not until the mid-to-late 20th century that researchers began to develop ways to quantify the role of rock strength in geomorphology (Bursztyn et al., 2015). There are two main groups of physical rules that have been developed in order to explain erosion in bedrock rivers. There are "process rules" and "reach-scale" rules. Process rules model bedrock channel erosion based on a singular erosional process such as the role of bedload impact on a channel, and reach-scale rules which focus on relationships between map scale features (such as stream discharge) and erosion rates. A majority of studies focus on reach-scale rules due to the difficulty of analyzing one singular process (Hancock et al., 1998). When studying the natural world, it is not often that contributing erosional factors are held constant in order to study one process.

One common equation used to study reach-scales rules is the Stream Power Law equation. This equation relates erosion rate (E) to erodibility (K), drainage area (A), and channel gradient (S) (Hancock et al., 1998; Bursztyn et al., 2015):

$$E = KA^{m}S^{n} \qquad \textit{Eq. 1}$$

The variables *m* and *n* are constants that are related to A and S, respectively. These constants vary as a function of erosion, sediment flux, bedrock erodibility, but the ratio of *m/n* should be around 0.5. This formula is relevant when assessing the role of rock strength in rates of erosion, and erosion rates are of chief importance when studying river valley development over time (Hancock et al., 1998). The variable K (erodibility) encompasses various rock properties, sediment properties, and erosional processes. Rock properties here is defined as the lithology of the rock, fracture spacing, fracture orientation, resistance, grain size, and minerals present. All of these influence the strength of the rock in various ways. For example, a highly fractured rock will have less strength than an intact massive rock.

From the equation, it can be inferred that lithology (and thus the strength of the rock) directly influences the erodibility of the bedrock. A higher K value means that the bedrock is generally less resistant to erosion, and a lower K value means that the bedrock is more resistant to erosion. To account for the higher and lower rock strengths, the equation shows that the slope of the channel (S) responds by having a steeper slope in strong rock, and a lower slope in weak rock when holding drainage area and uplift the same (Schanz and Montgomery, 2016).

Quantifying rock strength to determine its influence on river incision and valley form is a large endeavor (Goudie, 2016). When analyzing fluvial landforms to quantify rock strength, researchers often turn to the use of the Schmidt Hammer (SH) or the Equotip. Both of these devices measure hardness based on the rebound value of an impact onto the rock face. The

Schmidt Hammer has been used extensively in the field because of its ease of use, and relatively low impact on the rock itself. In one study measurements of rock strength using a Schmidt Hammer showed that channels tend to be narrower in areas of high strength (Allen et al., 2013).

Discontinuities in Rock

Fractures, joints, and bedding planes (commonly grouped together as discontinuities) have long been known to influence the way landforms develop over time. In 1905, G.K. Gilbert published a paper on the asymmetry of crest lines in the High Sierras. In this publication, Gilbert realized that in the heavily jointed granite, "the details of sculpture are greatly influenced". Using somewhat outdated terms, Gilbert is referring to the instability of the hillslopes in the Sierras (Scott and Wohl, 2019).

Scott and Wohl (2019) developed three primary rules that explain the characteristic ways in which discontinuities influence geomorphic processes and forms. They are as follows: (1) Spacing and orientation control erosion rate and style; (2) discontinuities that bound landforms influence erosion rate, style, and shape; and (3) variations in erosion rate control discontinuity propagation. Bedrock erodes primarily through four processes as describe by Hancock et al. (1998). These processes are abrasion, bed quarrying, cavitation, and hydraulic wedging. Oftentimes, these processes are working in conjunction with one another. Quarrying is of chief importance when considering the influence of fractures in rocks. In a bedrock river, quarrying of rocks is more rapid than abrasion when the joint spacing is close enough to allow blocks to be removed by the flow of a river. For blocks to be removed in this way, it is critical that they undergo a significant amount of weathering in what is known as a "pre-conditioning period". During this period, joints are spread apart through abrasion and hydraulic wedging (Hancock et al., 1998).

Hydraulic wedging is a term that entered the lexicon of geomorphic terms in 1998 in a paper published by Hancock et al. This process prepares blocks for quarrying by wedging transported clasts of preexisting rock into joints. There are two main ways that clasts are thought to be emplaced into a joint. The first way is through forceful emplacement when stream velocity is high enough to wedge a clast that is larger than a joint. The second way is through passive emplacement as a joint undergoes temporary widening. Joints temporarily widen by pressure fluctuations exerted by turbulent water flow (Hancock et al., 1998).

It is important to consider the scale at which discontinuities influence bedrock channel morphology. At the micro scale (mm to cm) discontinuities help to determine porosity, permeability, and susceptibility to chemical weathering. At the meso scale (cm to m), discontinuities play a larger role in that they help to focus weathering and differential erosion. At the micro scale, rock properties like mineralogy play a larger role in erosion over discontinuities. At the macro scale, regional joint patterns, structural variation, tectonics, and lithologic contacts play large roles. Initial weaknesses in lithology such as jointing can exacerbate erosion at meso and macro scales (Wohl, 1998).

Discontinuity spacing and orientation influences the structure of a wide variety of landforms including but not limited to hillslope relief, knickpoints, and channel width. Studies done on the relationship between discontinuities and the relief of landscapes are relatively numerous. Schmidt and Montgomery (1995) found that rock strength measurements in the lab far outpaced measurements of rock strength when discontinuities were considered. They found that fractured sandstones, siltstones, and shales all directly contributed to unstable valley forms. DiBiase et al. (2018) found that fracture density as well as grain size contributed to the unstable landscape relief in the northern San Jacinto Mountains and the eastern San Gabriel Mountains.

This study also found that along with a high uplift rate, fracturing accelerated the process of erosion. Loye et al. (2012) analyzed fracture networks and joint spacing using remote sensing techniques to explain the morphological development of landforms in alpine catchments. One of their main findings was that in multiple catchments, the potential for slope failure aligned with local joint systems.

One study on the development of knickpoints on a river in Indiana found that knickpoints are characterized by a step from jointed, highly resistant rock that overlies weaker units. The form of these knickpoints serves in large part to protect the weaker unit. The closer to the edge of the knickpoint, joints become progressively enlarged and bedding plane structures also widen. This serves to enhance the ease at which large blocks can be removed during flooding episodes (Miller, 1991).

When influencing the development of bedrock erosion, discontinuities control either vertical incision or channel width. Fracture density is of high importance in the overall development of channel width because densely fractured rock leads to a development of wider valleys. This can lead to differential erosional patterns along the same river channel (Scott and Wohl, 2019). Wohl (2008) showed evidence of this differential erosional pattern when analyzing bedrock jointing on the formation of straths in the Cache de la Poudre River in Colorado. The presence of sub-horizontal joints contributed to a lower rock mass strength. This lower rock mass strength facilitated lateral erosion. This lateral erosion contributed to the widening of the valley bottoms so that strath terraces could more easily form (Wohl, 2008).

Field Methods for Discontinuity Measurements

In 1978, the International Society for Rock Mechanics (ISRM) published a report that had the goal of standardizing methods to be used in the description of discontinuities in rock

masses. In this paper, various characteristics were selected to describe discontinuities. The characteristics that are of importance to this study and that will be expanded upon are orientation, density, spacing, and size. These are defined in Table 1 below.

Table 1: Discontinuity characteristic definitions synthesized from various texts.

Fracture Characteristic	***Definition***	***References***
Orientation	The orientation of a discontinuity can be adequately defined as the strike, dip, and dip direction.	ISRM (1978); Bieniawski, (1989); Priest, (1993)
Spacing	The distance between one discontinuity and another.	Priest and Hudson (1976); ISRM (1978); Bieniawski (1989); Priest (1993)
Density	The mean number of discontinuities per unit volume or length. In the literature referenced "frequency" is often used in place of density if the unit is length. This changes between different authors, and both terms are generally accepted to mean the same thing.	ISRM (1978); Bieniawski (1989); Priest (1993); Scott and Wohl (2019)
Size	Due to the difficulties of developing a model for discontinuity shape, it is common practice to consider discontinuities as 2D features. This is known as a discontinuity trace. A trace can be seen at outcrop where the discontinuity intersects with the rock face. The size is measured as the length of the trace.	ISRM (1978); Bieniawski (1989); Priest (1993)

All the above characteristics can be measured at a rock face using various scanline methods. The linear scanline method has been a common method to sample discontinuities in the field since the 1960's. Priest (1993) published *Discontinuity Analysis for Rock Engineering* where he details

the best practices for setting up a linear scanline survey. In general, a linear scanline survey involves pinning a measuring tape to a rock face with the goal of intersecting discontinuities with the tape. Each fracture is measured at its location along the tape in mm or cm. At each intersection of the tape and discontinuity, characteristics like orientation and size of the discontinuity are recorded. Scanline surveys benefit from their cost effectiveness and simplicity relative to the large amount of data that is collected.

Window sampling is also a common technique employed by geologists and geological engineers to investigate discontinuities (Priest, 1993). This involves setting up a rectangle directly on a rock face using measuring tapes. Once the setup is complete, discontinuity characteristics that are measured for the linear scanline are also measured for this type of survey. The main difference is that all discontinuities contained within the rectangle are measured, not just those that cross the tape. This type of survey has the benefit of minimizing orientation bias of discontinuities but can be rather difficult to setup depending on the field location and nature of the rock outcrop.

More recently, the circular scanline method put forth by Mauldon et al. (2001), Rohrbaugh et al. (2002) and expanded upon by Watkins et al. (2015) has been used. This method uses a circle drawn onto the outcrop using chalk and rope. This circle has a known radius of r. Once the circle is drawn, the number of fracture intersections with the edge of the circle (n), and the number of fracture terminations within the circle (m) are counted. Using the variables n and m, a series of equations can be used to determine fracture frequency and fracture size. This type of methodology suffers from the same general drawbacks as normal window sampling. Access to a rock outcrop to draw a circle onto it can be hazardous to the researcher and difficult to accomplish.

Rock Mass Classification Systems

Rock Quality Designation (RQD) is a method first devised in the 1960's that is used to describe the nature of a rock mass using rock cores collected during exploratory drilling operations (Deere and Deere, 1989). RQD is the proportion of borehole core that consists of intact lengths (not broken up by discontinuities) greater than or equal to 10 cm. RQD can be calculated using the following equation (Priest and Hudson, 1976):

$$RQD = 100 \sum_{i=1}^{n} x_i / L \qquad Eq.\ 2$$

The variable x_i is the i^{th} length of core greater than 10cm, L represents the length of the borehole, and n represents the number of lengths greater than 10 cm. Priest and Hudson (1976), Wines and Lilly (2002), and Choi and Park (2004) have all calculated RQD along linear scanlines instead of rock core and found that the equation holds true in that application. Andriani and Walsh (2007) have shown that implementing RQD into investigations of discontinuity spacing has application within a geomorphic context, specifically in helping to determine the susceptibility of erosion at exposed rock faces.

The Rock Mass Strength (RMS) index put forth by Selby (1980) is a common tool in geomorphological studies used to characterize the degree of weathering that has taken place on a rock face (Priest, 1993). It uses the following parameters: strength of intact rock, the state of weathering of the rock, the spacing, orientation, width, persistence and filling of discontinuities, and the movement of water within or out of the rock mass (ISRM, 1978). Similarly, the Rock Mass Rating system is a tool used in geomorphological studies as well as geotechnical work.

Utilizing only information obtained from rock core and scanlines to categorize an entire formation would be ill advised because data such as strength of the rock and groundwater

influences are not accounted for. To solve this problem, it is common practice to combine the values calculated from RQD equations into a broader classification scheme. The Rock Mass Rating System (RMR), proposed by Bieniawski (1973; 1989), utilizes RQD as one of its input parameters and has been used in engineering investigations, as well as investigations into slope stability. The RMR uses six parameters to give the rock mass a rating between 0 and 100; a lower rating represents unstable material. The six parameters are as follows:

1. Uniaxial compressive strength of rock material
2. Rock Quality Designation (RQD)
3. Spacing of Discontinuities
4. Condition of Discontinuities
5. Groundwater conditions
6. Orientation of discontinuities

Similarly, the RMR_B (RMR Basic) uses the first five parameters to classify a rock mass (Bieniawski, 1989).

LiDAR (Light Detection and Ranging) and Geologic Outcrop Models

The first published mention of LiDAR within a geologic context was by Schuster in the 1960s (Bellian et al., 2005). Since then, the use of LiDAR to help solve geologic problems has increased. In recent years, terrestrial LiDAR techniques have been used to aid in the development of 3D outcrop models. LiDAR technology functions similarly to sonar or radar, except that LiDAR uses light waves to measure distance between the device and the object to be scanned (Bellian et al., 2005). One of the benefits to using this technology is that much of the risk associated with creating a cross-section by hand is eliminated (Bellian et al., 2005). Many rock outcrops can be difficult to access due to drop offs, or they can have vertical walls that are

simply hard to reach. Terrestrial LiDAR scanning of rock faces allows for digital scans to be made of the rock face in question at a safe distance. In addition to enhanced safety, LiDAR scans allow the user to carry out detailed interpretation of data in the lab using a variety of software suites (McCaffrey et al., 2005). Users can also digitize surfaces directly onto the 3D image created by the scan to map stratigraphic contacts, discontinuities, tectonic structures, and weathering surfaces (McCaffrey et al., 2005).

Works Cited

Allen, G.H., Barnes, J.B., Pavelsky, T.M., and Kirby, E., 2013, Lithologic and tectonic controls on bedrock channel form at the northwest Himalayan front: Journal of Geophysical Research: Earth Surface, v. 118, p. 1806–1825, doi:10.1002/jgrf.20113.

Andriani, G.F., and Walsh, N., 2007, Rocky coast geomorphology and erosional processes: A case study along the Murgia coastline South of Bari, Apulia — SE Italy: Geomorphology, v. 87, p. 224–238, doi:10.1016/j.geomorph.2006.03.033.

Bellian, J.A., Kerans, C., and Jennette, D.C., 2005, Digital outcrop models: Applications of terrestrial scanning lidar technology in stratigraphic modeling: Journal of Sedimentary Research, v. 75, p. 166–176, doi:10.2110/jsr.2005.013.

Bieniawski, Z.T., 1989, Engineering rock mass classifications: a complete manual for engineers and geologists in mining, civil, and petroleum engineering: New York, Wiley, 251 p.

Braden, A., Ausbrooks, S., Mayfield, W., and Clark, J., 2003, Geologic Map of the Snowball Quadrangle, Searcy County, Arkansas: USGS Topographic, http://buffalorivergeoscience.org/maps (accessed October 2019).

Bursztyn, N., Pederson, J.L., Tressler, C., Mackley, R.D., and Mitchell, K.J., 2015, Rock strength along a fluvial transect of the Colorado Plateau – quantifying a fundamental control on geomorphology: Earth and Planetary Science Letters, v. 429, p. 90–100, doi:10.1016/j.epsl.2015.07.042.

Choi, S.Y., and Park, H.D., 2004, Variation of rock quality designation (RQD) with scanline orientation and length: a case study in Korea: International Journal of Rock Mechanics and Mining Sciences, v. 41, p. 207–221, doi:10.1016/S1365-1609(03)00091-1.

Deere, D.U., and Deere, D.W., 1989, Rock Quality Designation (RQD) After 20 Years, 102 p.

DiBiase, R.A., Rossi, M.W., and Neely, A.B., 2018, Fracture density and grain size controls on the relief structure of bedrock landscapes: Geology, v. 46, p. 399–402, doi:10.1130/G40006.1.

Gilbert, G.K., 1877, Report on the Geology of the Henry Mountains, *in* US Governement Printing Office, Washington, D.C., p. 160.

Goudie, A.S., 2016, Quantification of rock control in geomorphology: Earth-Science Reviews, v. 159, p. 374–387, doi:10.1016/j.earscirev.2016.06.012.

Hancock, G., Anderson, R., and Whipple, K., 1998, Beyond Power: Bedrock River Incision Process and Form, *in* Tinkler, K. and Wohl, E. eds., Rivers Over Rock: Fluvial Processes in Bedrock Channels, Washington, DC, American Geophysical Union, Geophysical monograph 107, p. 133–151, doi:10.1029/GM107p0035.

Hudson, M.R., and Murray, K.E., 2003, Geologic Map of the Ponca Quadrangle, Newton, Boone, and Carroll Counties. Arkansas: USGS Topographic, https://pubs.usgs.gov/mf/2003/mf-2412/.

ISRM, 1978, International society for rock mechanics commission on standardization of laboratory and field tests: International Journal of Rock Mechanics and Mining Sciences & Geomechanics Abstracts, v. 15, p. 319–368, doi:10.1016/0148-9062(78)91472-9.

Keen-Zebert, A., Hudson, M.R., Shepherd, S.L., and Thaler, E.A., 2017, The effect of lithology on valley width, terrace distribution, and bedload provenance in a tectonically stable catchment with flat-lying stratigraphy: Earth Surface Processes and Landforms, v. 42, p. 1573–1587, doi:10.1002/esp.4116.

Kuniansky, E.L., 2011, U.S. Geological Survey Karst Interest Group Proceedings, Fayetteville, Arkansas, April 26-29, 2011: U.S. Geological Survey Scientific Investigations Report USGS Numbered Series 2011–5031, 218 p., http://pubs.er.usgs.gov/publication/sir20115031 (accessed October 2019).

Loye, A., Pedrazzini, A., Theule, J.I., Jaboyedoff, M., Liébault, F., and Metzger, R., 2012, Influence of bedrock structures on the spatial pattern of erosional landforms in small alpine catchments: Earth Surface Processes and Landforms, v. 37, p. 1407–1423, doi:10.1002/esp.3285.

Mauldon, M., Dunne, W.M., and Rohrbaugh, M.B., 2001, Circular scanlines and circular windows: new tools for characterizing the geometry of fracture traces: Journal of Structural Geology, v. 23, p. 247–258, doi:10.1016/S0191-8141(00)00094-8.

McCaffrey, K.J.W., Jones, R.R., Holdsworth, R.E., Wilson, R.W., Clegg, P., Imber, J., Holliman, N., and Trinks, I., 2005, Unlocking the spatial dimension: digital technologies and the

future of geoscience fieldwork: Journal of the Geological Society, v. 162, p. 927–938, doi:10.1144/0016-764905-017.

Miller, J.R., 1991, The influence of bedrock geology on knickpoint development and channel-bed degradation along downcutting streams in south-central Indiana: The Journal of Geology, v. 99, p. 591–605, doi:10.1086/629519.

Priest, S.D., 1993, Discontinuity Analysis for Rock Engineering: Dordrecht, Springer Netherlands, doi:10.1007/978-94-011-1498-1.

Rohrbaugh, M.B., Dunne, W.M., and Mauldon, M., 2002, Estimating fracture trace intensity, density, and mean length using circular scan lines and windows: AAPG Bulletin, v. 86, p. 2089–2104, doi:10.1306/61EEDE0E-173E-11D7-8645000102C1865D.

Selby, M.J., A rock mass strength classification for geomorphic purposes: with tests from Antarctica and New Zealand: Zeitschrift für Geomorphologie Stuttgart, v. 24, p. 31-51.

Schanz, S.A., and Montgomery, D.R., 2016, Lithologic controls on valley width and strath terrace formation: Geomorphology, v. 258, p. 58–68, doi:10.1016/j.geomorph.2016.01.015.

Schmidt, K.M., and Montgomery, D.R., 1995, Limits to relief: Science, v. 270, p. 617–620.

Scott, D.N., and Wohl, E.E., 2019, Bedrock fracture influences on geomorphic process and form across process domains and scales: Bedrock Fracture Influences on Geomorphology: Earth Surface Processes and Landforms, v. 44, p. 27–45, doi:10.1002/esp.4473.

Watkins, H., Bond, C.E., Healy, D., and Butler, R.W.H., 2015, Appraisal of fracture sampling methods and a new workflow to characterize heterogeneous fracture networks at outcrop: Journal of Structural Geology, v. 72, p. 67–82, doi:10.1016/j.jsg.2015.02.001.

Wines, D.R., and Lilly, P.A., 2002, Measurement and analysis of rock mass discontinuity spacing and frequency in part of the Fimiston Open Pit operation in Kalgoorlie, Western Australia: a case study: International Journal of Rock Mechanics and Mining Sciences, v. 39, p. 589–602, doi:10.1016/S1365-1609(02)00003-5.

Wohl, E., 1998, Bedrock Channel Morphology in Relation to Erosional Processes, *in* Tinkler, K.J. and Wohl, E.E. eds., Rivers over rock: fluvial processes in Bedrock channels, Washington, DC, American Geophysical Union, Geophysical monograph 107, p. 133–151.

Wohl, E., 2008, The effect of bedrock jointing on the formation of straths in the Cache la Poudre River drainage, Colorado Front Range: Journal of Geophysical Research, v. 113, p. F01007, doi:10.1029/2007JF000817.

Z. T. Bieniawski, 1973, Engineering Classification of Jointed Rock Masses: Civil Engineer in South Africa, v. 15.

Chapter 3: Manuscript for Submission

Introduction

In his seminal study of the geology of the Henry Mountains, G. K. Gilbert (1877) discussed erosional processes that fundamentally changed how many geomorphologists study landforms and landscape change. He proposed that there are three main conditions that affect the speed at which rock erodes. These are declivity, character of the rock, and climate. The "character of the rock" in this context simply means the strength of the rock that is being eroded. Gilbert (1877) found that hard rocks have a higher resistance to erosional forces than soft rocks, and his work focused largely on a qualitative approach to studying how rock strength influences the development of landscapes. Contemporaries of Gilbert took a qualitative approach as well, with John Wesley Powell writing of the Colorado River in 1895: "Along its course where the rocks are hard, the stream is narrow and swift, with rapids and falls; where the rocks are soft, it is wide and quiet." (Bursztyn et al., 2015).

It was not until the mid-to-late 20th century that researchers began to develop ways to quantify the role of rock strength in geomorphology (Bursztyn et al., 2015). There are two main groups of physical rules that have been developed to quantitatively explain erosion in bedrock rivers. There are "process rules" and "reach-scale" rules. Process rules model bedrock channel erosion based on a singular erosional process such as the role of bedload impact on a channel. Reach-scale rules focus on relationships between map-scale features (such as stream discharge) and erosion rates. A majority of studies focus on reach-scale rules due to the difficulty of analyzing one singular process (Hancock et al., 1998). Contributing erosional factors are usually not held constant so that one process can be studied. Therefore, determining reach-scale rules for

a given catchment area serves as a comprehensive way to explain the processes that shape landforms.

Fractures, joints, and bedding planes (commonly grouped together as discontinuities) have long been known to have influence on the way landforms develop over time. In 1905, G.K. Gilbert published a paper on the asymmetry of crest lines in the High Sierras. In this publication, Gilbert realized that in the heavily jointed granite, "the details of sculpture are greatly influenced". Using somewhat outdated terms, Gilbert is referring to the instability of the hillslopes in the Sierras (Scott and Wohl, 2019).

Discontinuity characteristics influence the structure of a wide variety of landforms including but not limited to hillslope relief, knickpoints, and channel width. DiBiase et al. (2018) found that fracture density as well as grain size contributed to the unstable landscape relief in the Northern San Jacinto Mountains and the Eastern San Gabriel Mountains. Loye et al. (2012) analyzed fracture networks and joint spacing using remote sensing techniques to explain the morphological development of landforms in alpine catchments. One of their main findings was that in multiple catchments, the potential for slope failure aligned with local joint systems.

The objective of this study is to investigate the spacing, density, orientation, and size of fractures and other discontinuities present within two primary formations of the study area. In addition, a comprehensive geomechanical classification of the lithologies in the study area derived from scanline measurements are used to draw conclusions about the stability of these formations. Combining remote sensing and field-based methods will serve to answer the question: How do fractures and other discontinuities measured at outcrops influence the erosional processes that shape the morphology of river valleys composed of heterogeneous lithologies in areas of low tectonic activity?

Study Area

The Buffalo National River Watershed (BNRW) is located at the southern extent of the Ozark Dome, a Paleozoic uplift that developed in the foreland basin during the Ouachita Orogeny. The Ozark Dome is separated by well-developed escarpments into three distinct physiographic provinces; these are the Salem, Springfield, and Boston Mountain plateaus seen in Figure 1 (Quinn, 1958; Keen-Zebert et al., 2017). Within the BNRW, the Buffalo National River (BNR) incises through a series of sedimentary layers ranging from Ordovician to Mississippian in age that exhibit differential erosional resistance. Reaches of the BNR composed primarily of Ordovician-aged strata have comparatively wider valleys than reaches composed of Mississippian-aged strata. Previous studies in the BNR have focused on measuring mechanical erosional resistances through Schmidt Hammer (SH) measurements and abrasion mill experiments, while chemical erosional resistance was evaluated using decarbonation methods (Keen-Zebert et al., 2017; Heidner, 2019). Keen-Zebert et al. (2017) and Heidner (2019) found that both the Boone and Everton Formations exhibit similar mechanical resistance and concluded that a primary cause of the varying valley width at different reaches along the river was due to the higher solubility of the Boone Formation over the Everton. Research by Keen-Zebert et al. (2017) and Heidner (2019) in the BNR confirms Gilbert's conclusion that the strength of lithology is one of the primary controls affecting the style of erosion, but it also leaves room to further explore the role of how fractures and other discontinuities influence the strength of the Boone and Everton. While it is clear lithology is of importance to valley form, it is yet unclear how the characteristics of *in situ* fractures and other discontinuities of the variable lithologies exposed along the BNR influence erosional processes.

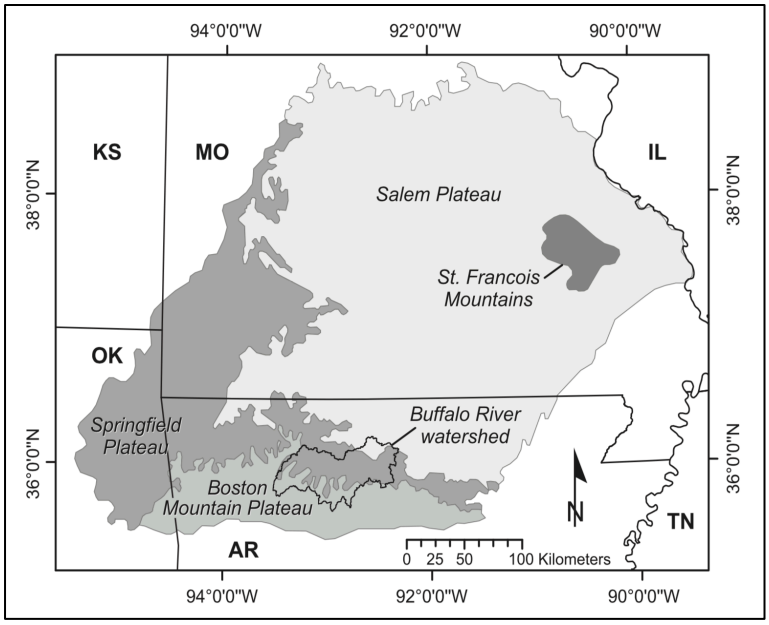

Figure 1: Map of the Ozark physiographic province. The study area is outlined in black at the southern extent of the map; from Keen-Zebert et al. (2017).

Stratigraphy

The BNR meanders primarily through the Springfield Plateau and the Boston Mountain Plateau, exposing nearly 500 m of sedimentary rock layers (Keyes, 1901; Purdue, 1901; Kuniansky, 2011). The exposed strata are gently dipping and are early to late Paleozoic in age, specifically, Ordovician, Mississippian, and Pennsylvanian (Kunianksy, 2011; Keen-Zebert, 2017). Deposition is thought to have continued throughout the Devonian and Silurian, but all the Devonian and much of the Silurian is missing from the geologic record (Smith, 2004). The majority of these clastic and carbonate sedimentary rocks were deposited in shelf-marine, near-shore marine, or fluvial environments (Mcknight, 1935; Kuniansky, 2011; Keen-Zebert et al., 2017).

This study focuses on the Everton and Boone formations, the two primary formations exposed at river level in the BNR. A 30-m tall section of the Ordovician Everton Formation, called Roark Bluff, is exposed on a meander of the Buffalo River (Figures 2A and 3). At the base

of the exposed bluff are terrace deposits of Quaternary gravels and sands. The thickness of these Quaternary deposits is no more than 1.5 m as mapped. Above the Quaternary gravels and sands there is a section of limestone, sandstone, and dolomite. The Everton Formation above these limestones, sandstones, and dolomites is largely composed of the Newton Sandstone member. This unit is known for forming large bluffs along the river, and is mainly composed of well-rounded, fine to medium-grained quartz arenites. The Newton Sandstone has a variable thickness of about 27.5 – 30.5 m (Hudson and Murray, 2003). Above the Newton Sandstone Member, the Upper Everton Formation is mainly composed of dolostones and limestones. There is also sandstone, cemented with calcite or dolomite, present in this unit (Hudson and Murray, 2003).

White Bluff is an exposed section of the Mississippian Boone Formation located farther east of Roark Bluff (Figures 2B and 3). This formation has a thickness of about 30.5 m and is composed largely of carbonate rocks. Coarse-grained fossiliferous limestones are interbedded with nodules and bedded chert. Springs and sinkholes, resulting from erosion of carbonate rocks within the formation, are abundant in the Boone Formation. The St. Joe Limestone member is a part of the Boone Formation, and this member is a medium-grained, thin-bedded limestone commonly found with crinoid fossils. The St. Joe member also has a basal sandstone unit that is medium-grained, moderately sorted, and well to sub-rounded (Braden et al., 2003).

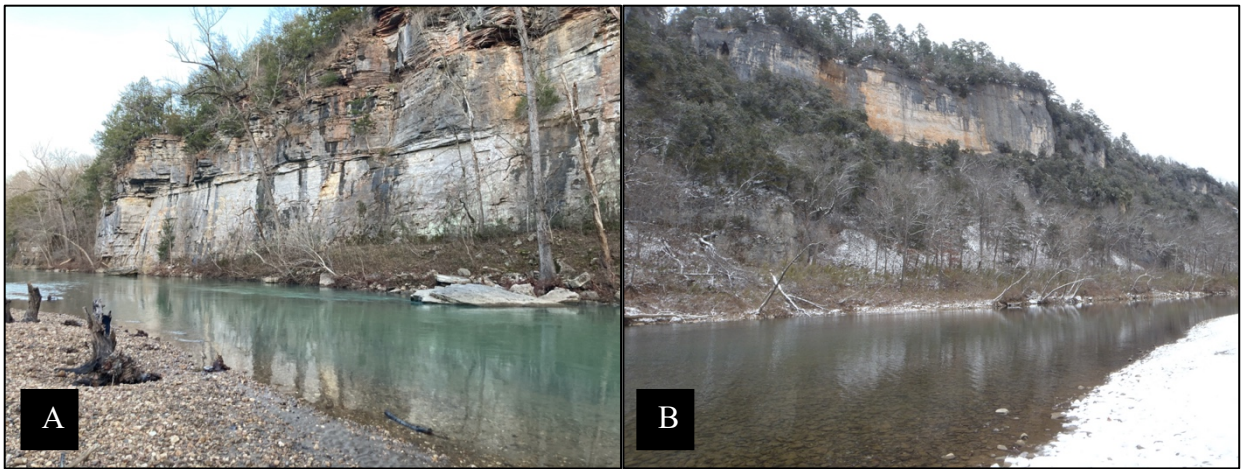

Figure 2: Panel A shows a picture of Roark Bluff, an exposed section of the Everton Formation, and Panel B shows a picture of White Bluff, an exposed section of the Boone Formation.

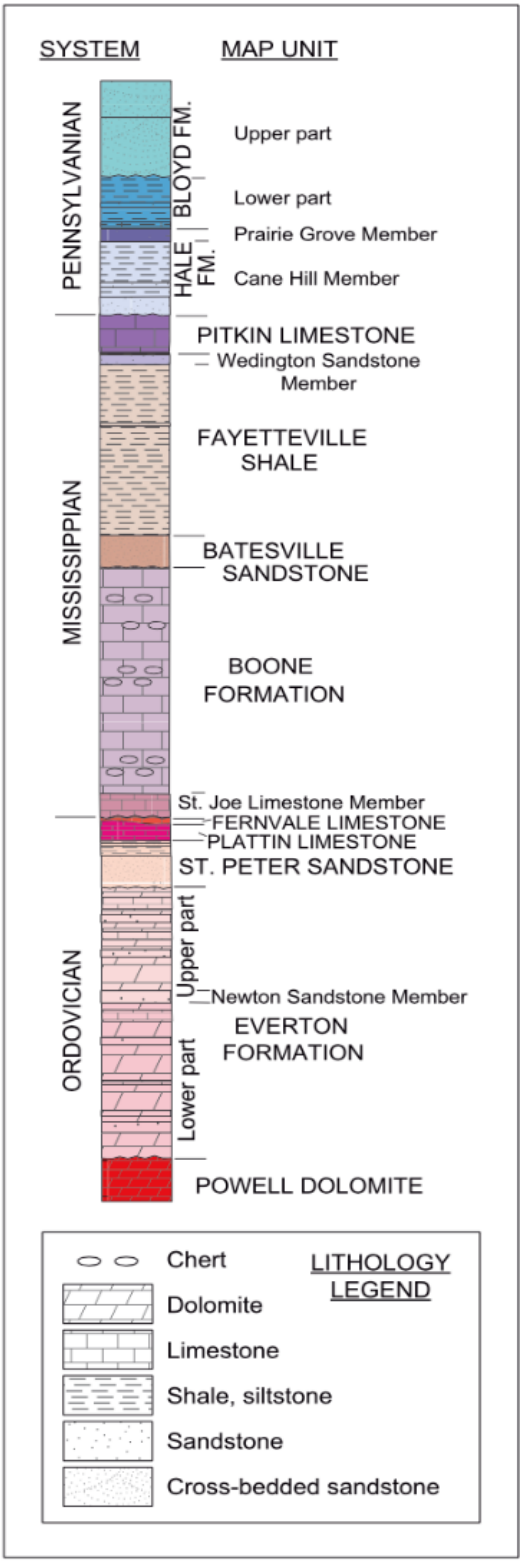

Figure 3: Stratigraphic column of the study area. There is an unconformity present between the Everton and Boone formations. Within the study area, there is no deposition during Devonian time and very little deposition during the Silurian; from Keen-Zebert et al. (2017).

Morphologic Setting

The BNR has been separated into four different lithologic reaches. Two of these reaches incise the Everton Formation, and two of them incise the Boone Formation. These reaches, and their location in the watershed, can be seen in Figure 4. Reach 1 and 3 incise the Boone and reaches 2 and 4 incise the Everton. These lithologic reaches were defined based on the prominent lithology of the lower valley walls at river level. Transitions between reaches are generally gradational, except for the transition between Reach 2 and Reach 3. Between these two reaches lies the Horn Mountain Fault, and here the Boone Formation is brought back to the surface (Keen-Zebert et al, 2017; Heidner, 2019).

Channel sinuosity has also been observed to be different among reaches of the Boone and Everton Formations. When the channel meanders from Boone Formation reaches to Everton Formation reaches, the sinuosity of the channel decreases. In areas of the Everton where the valley narrows, the channel becomes entrenched. Lateral channel migration is restricted by the more resistant Everton Formation. This relationship can be seen clearly by looking at the map in Figure 4. The transition between Reach 3 and Reach 4 is shown by a change in lithology, and a marked decrease in sinuosity of the channel (Keen-Zebert, 2017; Heidner, 2019).

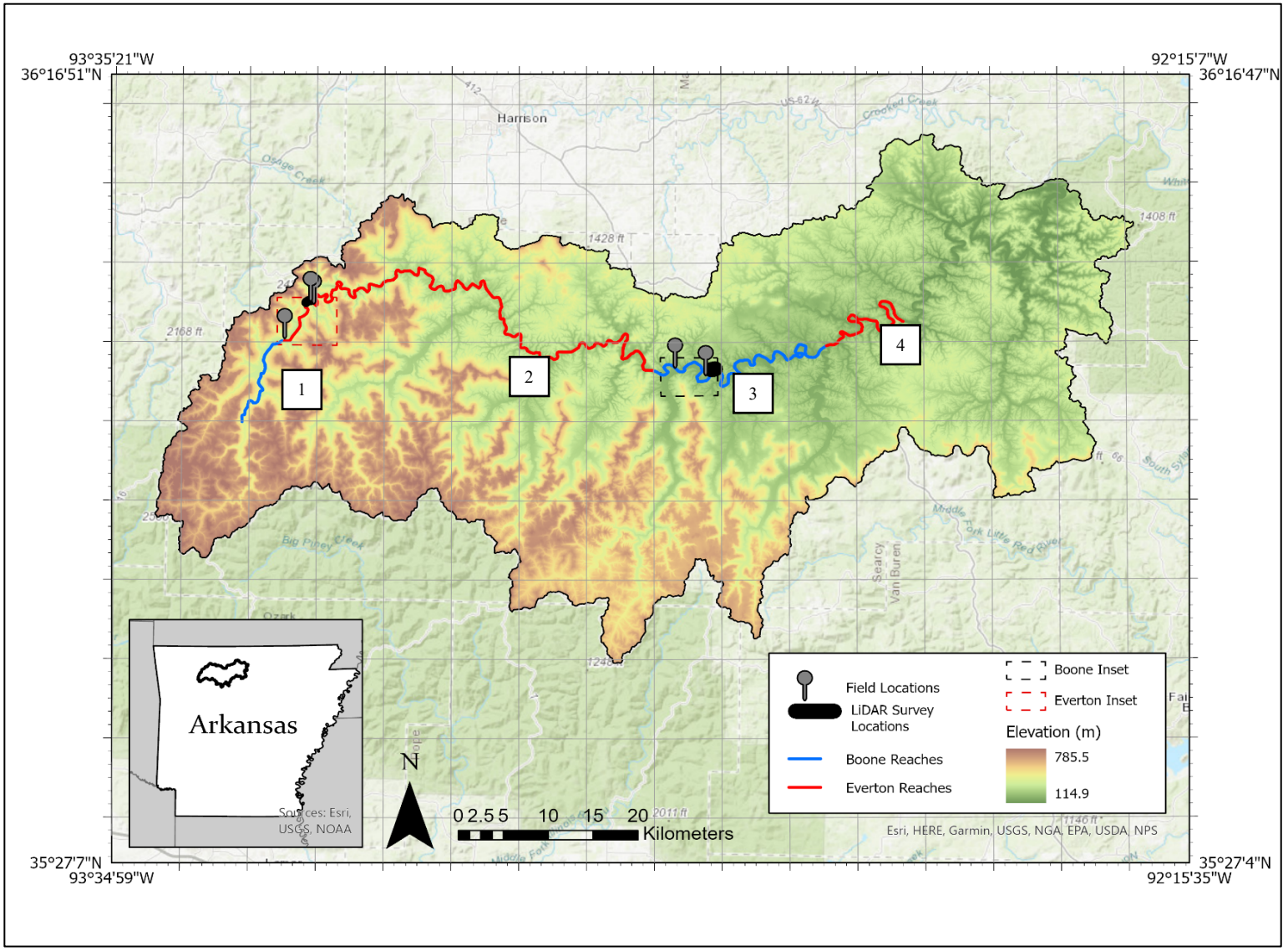

Figure 4: The BNRW is shown with elevation data created from 1-m DEM acquired from the Arkansas GIS Office. Locations of field surveys and LiDAR surveys are displayed, as well as lithologic reaches determined by Keen-Zebert et al. (2017) numbered 1-4. Inset

maps are provided for Boone study locations and Everton study locations in Figure 5 and 6. Background topographic data acquired from ESRI, Garmin, USGS, NGA, EPA, USDA, and NPS. Arkansas inset map data acquired from the United States Census Bureau.

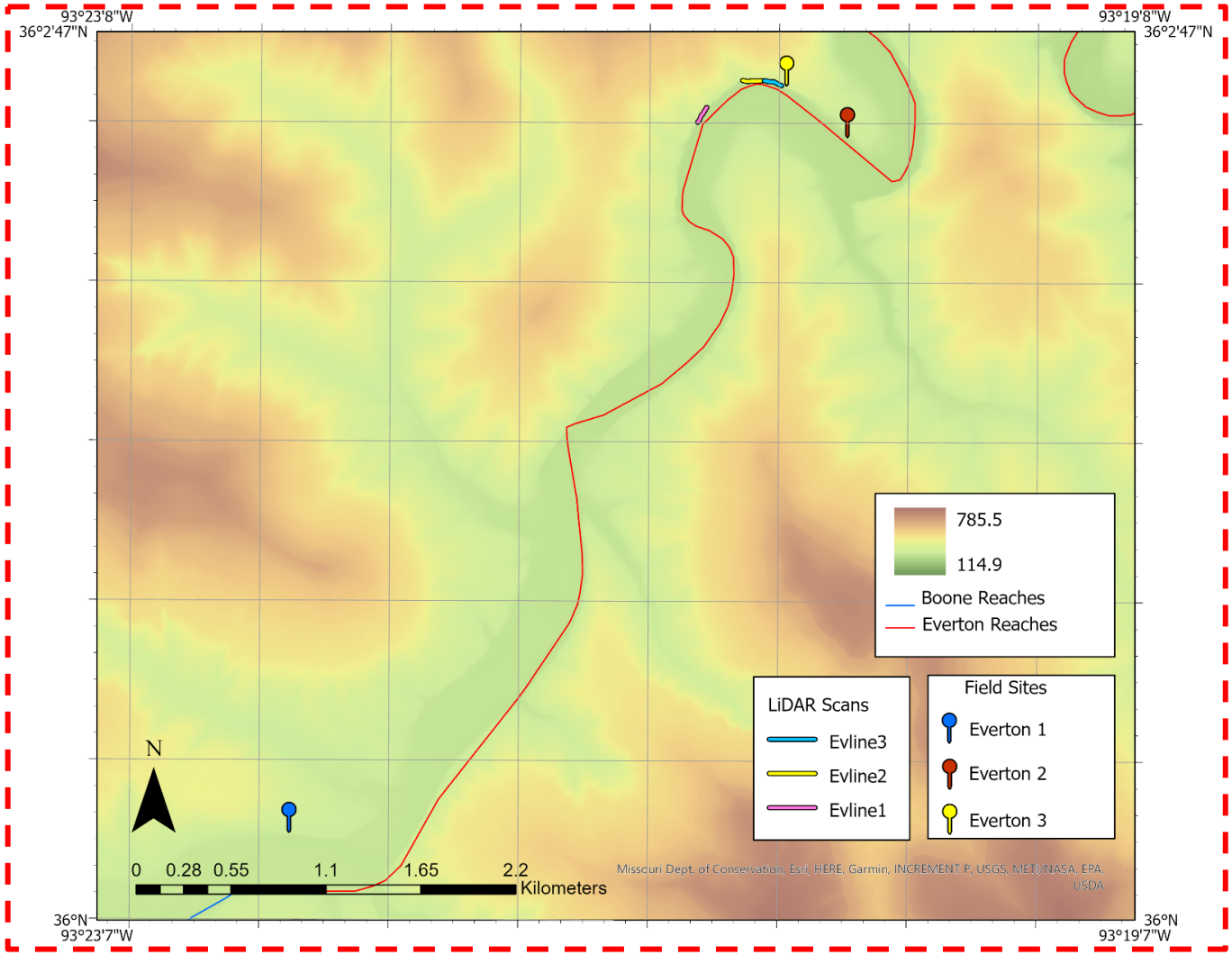

Figure 5: Inset map from Figure 4 showing field and LiDAR survey locations for the Everton Formation.

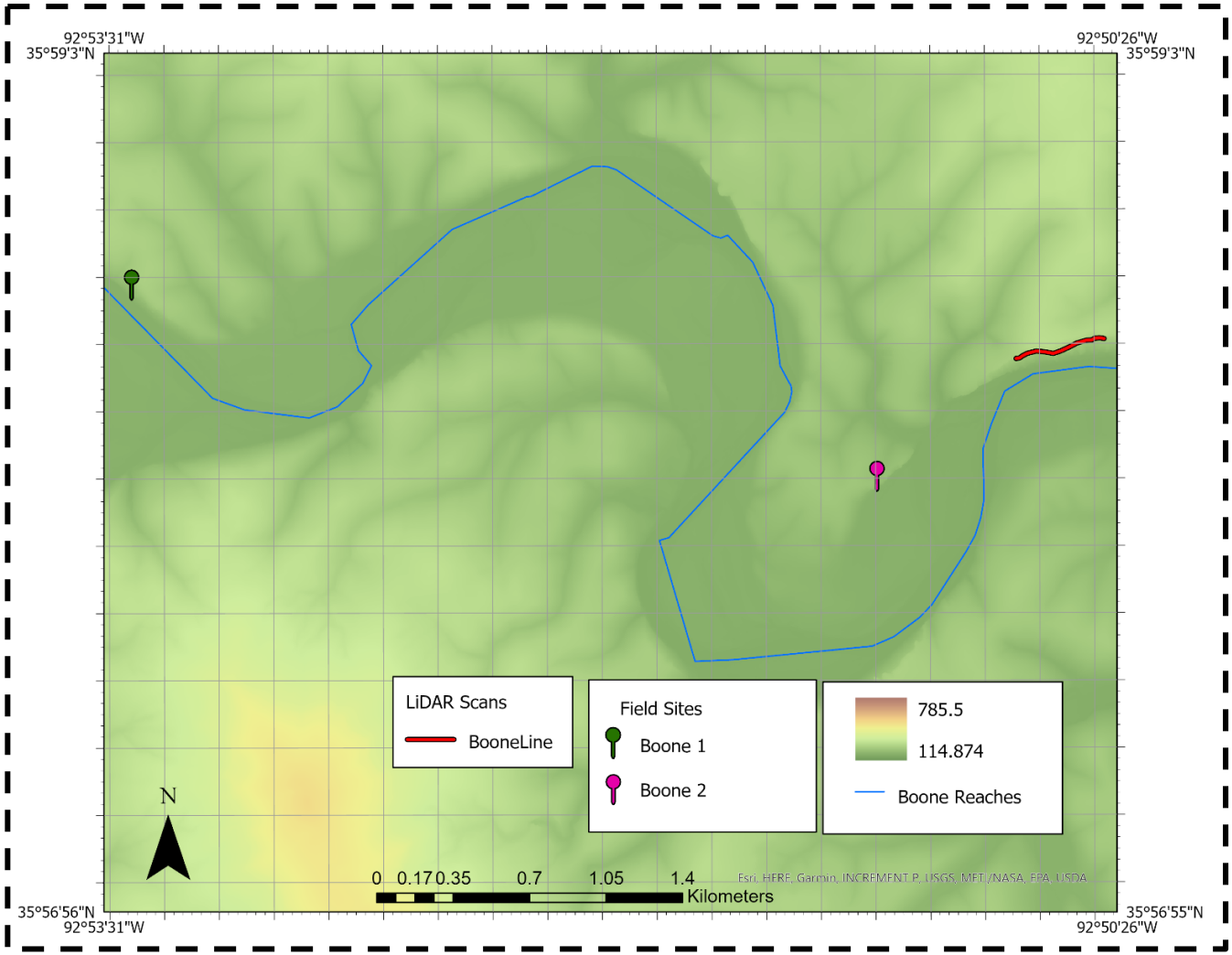

Figure 6: Inset map from Figure 4 showing field and LiDAR survey locations for the Boone Formation

Methodology

An investigation into the geologic structure of the Boone and Everton formations involved a combination of various methods detailed herein. LiDAR scans of the Boone Formation at White Bluff and Everton Formation at Roark Bluff were analyzed for orientation data using Split-FX and Leica® Cyclone. Field investigations of various fracture and discontinuity characteristics were carried out using linear scanlines. The orientation data collected from field and remote sensing methods were compiled into equal-area Schmidt Nets, and these were used to identify prominent fracture sets for each formation. Finally, the fracture sets and remaining discontinuity characteristics calculated through remote sensing and field methods were synthesized as input parameters into the RMR_B (Basic Rock Mass Rating) classification system to complete an evaluation of the strength of the rock mass for the Boone and Everton Formations.

Remote Sensing and LiDAR Methods

Leica® Cyclone was used to prepare the point clouds to be transferred to Split-FX for fracture and discontinuity identification. While Cyclone is not designed to analyze point clouds for discontinuity data, it remains a useful tool for the manipulation of them. To correctly identify fractures within Split-FX, point clouds need to be free of trees, shrubs, and other objects. All initial scans of the BNR were assessed for areas of maximum outcrop exposure, and for the Boone Formation this resulted in one area that was acceptable for analysis. For the Everton Formation, this resulted in three different areas of the point cloud that were acceptable. Only one area of the initial scan was acceptable for the Boone Formation because when the scan was completed, much of it did not capture enough of the rock face. The scan was distorted by trees, shrubs, and other objects that made analysis difficult. Once this selection process was complete,

the point clouds were extracted from Cyclone for use in Split-FX. Split-FX allows the user to identify fractures and other discontinuities as "fracture traces" and add them to the point cloud. The process by which this is done can be seen in an example from the scan of Roark Bluff in Figure 7.

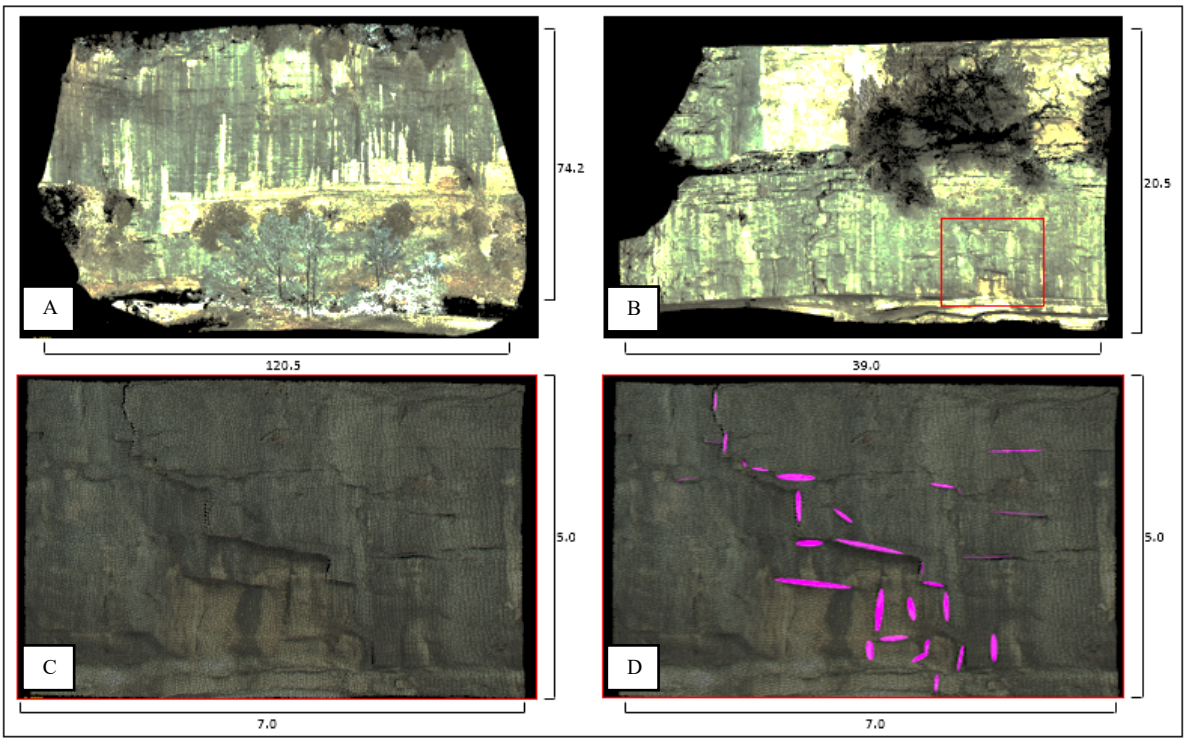

Figure 7: Sample process of inputting fracture traces into Split-FX. Panel A shows a scan of Roark Bluff before initial processing. Panel B shows a selection from the same scan that has been cleared of trees and other miscellaneous points that inhibit analysis. Panel C is the red box from Panel B showing clearly identifiable fractures in the rock mass. Finally, Panel D shows a selection of fracture traces added to the point cloud. Scale bar units are in meters.

Field Methods and Rock Mass Rating

Fractures and other discontinuities in the field were sampled using the scanline method outlined by Priest (1993). A scanline is simply a measuring tape pinned to the surface of a rock outcrop. Discontinuities that cross this tape are noted at the point they cross, and then characteristics such as strike, dip, dip direction, length above scanline, and length below scanline are recorded. In total, five locations were chosen to sample discontinuity characteristics using

linear scanlines. Three scanlines were put up at outcrops of the Everton Formation in Reach 2, and two scanlines were put up at outcrops of the Boone Formation in Reach 3. The locations of all field surveys conducted are indicated in Figures 5 and 6.

Using data collected at each scanline and data provided from previous studies regarding rebound (R) values for the Boone and Everton Formation, a classification of rock strength using the Basic Rock Mass Rating system (RMR_B) after Bieniawski (1989) was completed. This classification scheme determines rock quality based on the following parameters: (1) Uniaxial Compressive Strength (UCS) measured in MPa. (2) Rock Quality Designation (RQD) given in percent out of 100. (3) Spacing measured in cm. (4) Condition of fractures and other discontinuities. (5) General groundwater conditions assessed at outcrop. Points are allotted for each parameter, and then they are summed to get a total point value. The maximum value that a rock mass can have is 100, and a higher point value indicates that the rock mass is in overall better condition.

UCS was converted from Schmidt Hammer Type N measurements collected for the Boone and Everton Formation across the study area in a previously conducted field investigation. Schmidt Hammers evaluate rock hardness and strength non-destructively by delivering a 2.207 Nm impact to a rock face. This generates a rebound value (R) that can be converted to UCS. R values were converted to UCS following the equation derived by Katz et al. (2000). Katz et al. (2000) converted R to UCS based on measurements of sandstones and limestones that have similar R values to the Boone and Everton Formation. The equation used to convert R to UCS is:

$$UCS = 2.208e^{0.067R} \qquad \textit{Eq. 1}$$

RQD is defined as the percentage of length of a given borehole that consists of intact pieces that are greater than or equal to 10 cm. It was developed by Deere and Deere (1989) for

use in borehole measurements but has since been applied to scanlines to good effect (Priest, 1993; Choi and Park, 2004; Andriani and Walsh, 2007). The equation used to calculate RQD is:

$$RQD = 100 \sum_{i=1}^{n} x_i / L \qquad Eq.\ 2$$

For use in scanlines, x_i is the length of rock along a scanline between two fractures greater than 10 cm, L represents the length of the scanline, and n represents the number of lengths greater than 10 cm.

Condition of fractures and groundwater conditions were also assessed at outcrop. Based on the guidelines proposed for the RMR_B, the condition of each fracture was assessed semi-quantitatively, and depends upon criteria such as roughness, aperture, and weathering of the rock face. Groundwater conditions can be assessed based on joint water pressure and inflow per 10 m, but the RMR_B also allows for these conditions to be qualitatively assessed at outcrop. This assessment is carried out based on the apparent wetness of the outcrop and fractures, and it includes five classifications ranging from "completely dry" to "flowing". A study area classified as "completely dry" would receive more points than a study area classified as "flowing".

In addition to the parameters necessary for the RMR_B classification scheme, the spacing, density, and size of fractures were all calculated according to Priest (1993). Spacing is a measure of the distance between fractures on a scanline, and density is a measure of the number of fractures per unit length. Size is challenging to quantify using scanline methods because usually only the linear trace of the fracture intersects with the rock face. In this case, the size of a fracture is defined here as the length of the fracture above and below a scanline.

Orientation Data

Plotting the dip direction and dip of a fracture as a pole on equal-area Schmidt plots allows for trends in the data to be recognized (Turner et al., 2006). All orientation data collected

were plotted using the program Orient (Vollmer, 2015). Once the orientation data have been plotted, contouring is used to determine the density of poles plotted. In general, areas of densely plotted poles coincide with unique fracture sets that have a characteristic orientation. Plots were contoured according to the method developed by Vollmer (1995). Once contours were calculated, clusters of similar orientations can be identified by means of the clustering algorithm developed by Vollmer (1990). This method involves some subjective input from the user because the algorithm requires the user to input the approximate number of clusters. Mean orientation of fracture sets were also calculated and plotted on the Schmidt plots after cluster analysis was performed.

Results

Fracture Orientation Sets

As mentioned earlier, fracture sets for the Boone and Everton Formation have been identified using equal-area Schmidt plots. For the Boone Formation, those measurements taken along a scanline show three distinct clusters of fractures (Figure 8). In total, 74 fracture orientations were recorded across two field sites. These fractures dip to the north, northeast, and northwest. There were 57 fracture orientations recorded for the Boone Formation using Split-FX, and there are two clusters. These fractures dip to the north and to the northwest.

Combining the fractures taken at outcrop and measured remotely gives a full sense of fracture orientations for the Boone Formation. Four sets were identified from the final combined Schmidt plot. Set 1 is interpreted as the bedding plane of the formation, as it has a very low dip amount compared to the other three sets. For the purposes of this analysis, the bedding plane is included as a set because bedding planes are commonly considered discontinuities when they

serve to destabilize the rock mass. This is often the case in sedimentary rocks. Schmidt plots for the Boone Formation are shown in Figure 8, and mean orientation for each fracture set is listed in Table 1.

Table 1: Mean set orientations for the Boone and Everton Formations.

Fracture Set Mean Orientations (Dip Direction / Dip)		
Everton	Set 1	339.6° / 2.9°
	Set 2	283.0° / 81.8°
	Set 3	50.6° / 89.0°
	Set 4	335.8° / 87.8°
Boone	Set 1	347.5° / 8.6°
	Set 2	58.8° / 76.4°
	Set 3	357.0° / 82.7°
	Set 4	302.6° / 71.8°

Out of three scanline surveys conducted for the Everton Formation, a total of 81 fracture orientations were recorded. The Schmidt plot for just those recorded in the field show two different clusters. The fractures recorded here dip largely to the northwest, while some of them dip to the southeast. There were considerably more fractures measured using Split-FX for the Everton Formation than the Boone, primarily due to the Everton formation scan being of higher quality. In total, there are three clusters identified out of a total of 291 fractures (Figure 9). These generally dip to the northwest and to the northeast. Combining fractures taken at outcrop and measured remotely for the Everton Formation ultimately reveals four distinct fracture sets. Set 1 is the bedding plane, and the mean orientations of each set can be seen in Table 1. Schmidt plots for the Everton are shown in Figure 9. Fracture set 2 for both the Boone and Everton Formations contain a greater number of fractures per set, making them the dominant set for each formation.

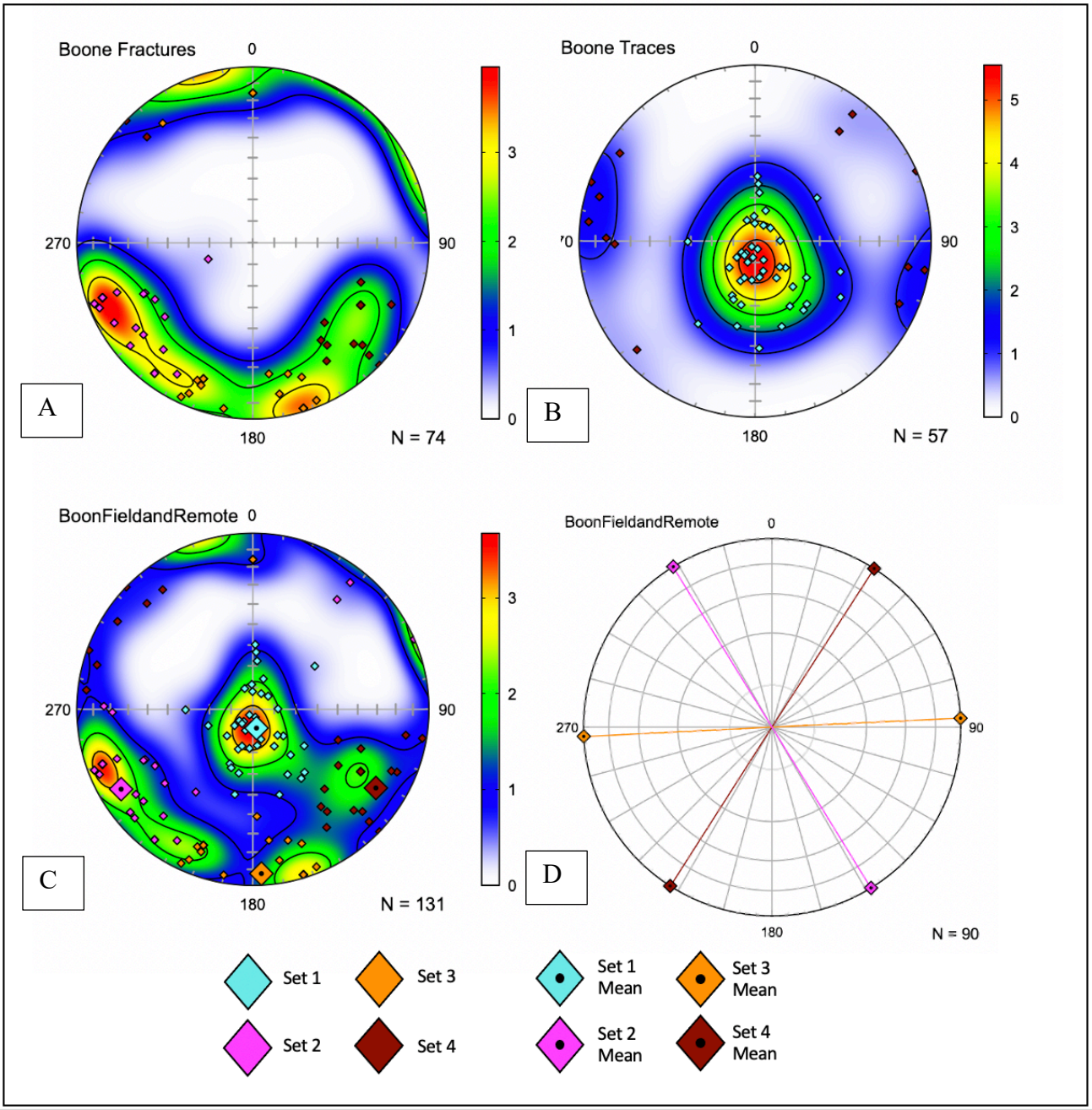

Figure 8: Schmidt plots for the Boone Formation. Plot A shows fractures sampled in the field, Plot B shows those identified in Split-FX, and Plot C shows all fractures in one plot. Plot D is a circular diagram showing the mean strikes for each fracture set. Each set is shown as a different colored diamond, while the mean for each set is shown as a diamond with a dot in the middle. Contour interval is 1 multiple of uniform density (MUD), and the color gradient scale to the right of each plot shows the MUD as well. Red represents a higher density of poles plotted, while light blue indicates a low density of poles.

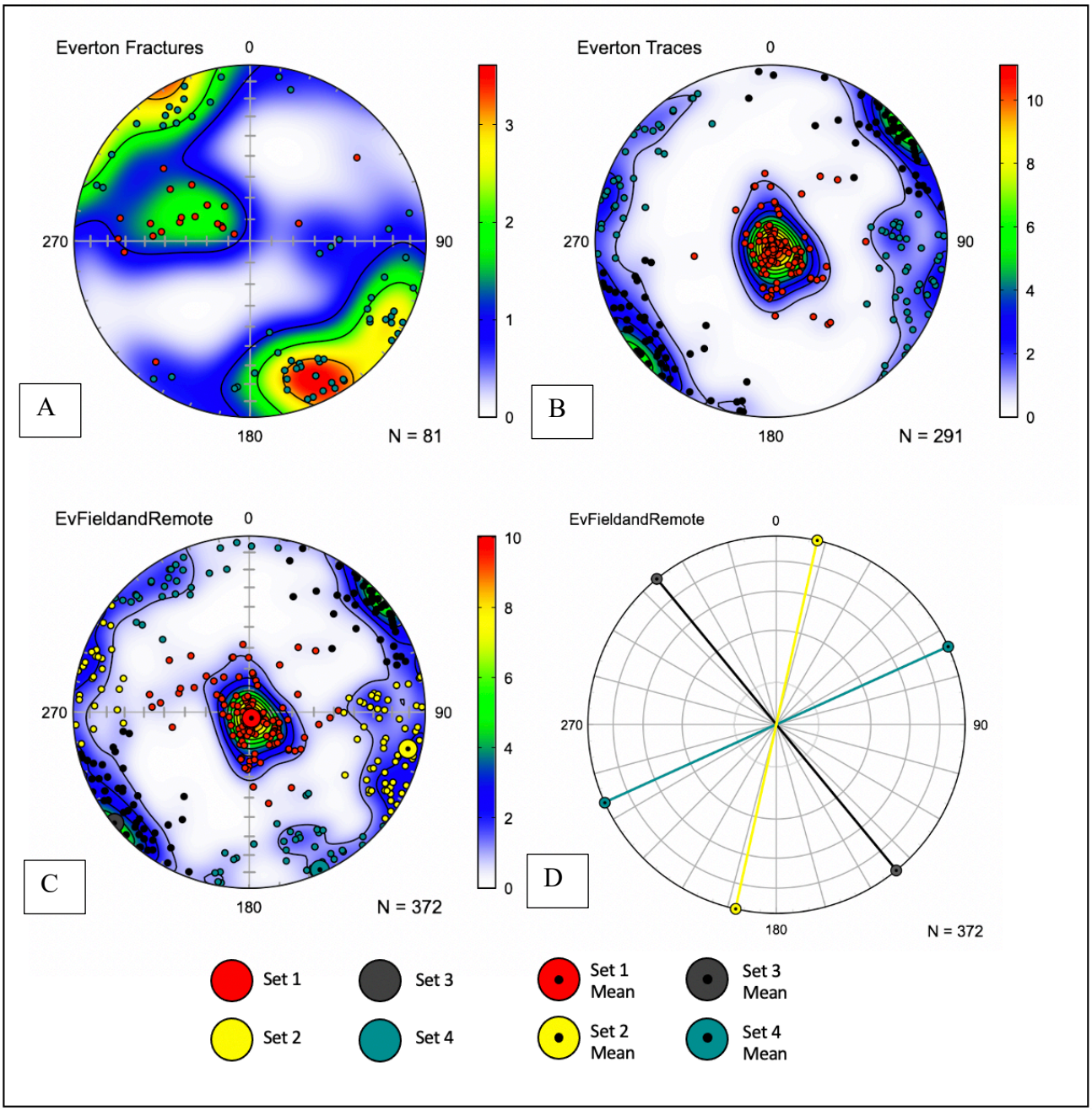

Figure 9: Schmidt plots for the Everton Formation. Plot A shows fractures sampled in the field, Plot B shows those identified in Split-FX, and Plot C shows all fractures in one plot. Plot D is a circular diagram showing the mean strikes for each fracture set. Each set is shown as a different colored circle, while the mean for each set is shown as a circle with a dot in the middle. Contour interval is 1 multiple of uniform density (MUD), and the color gradient scale to the right of each plot shows the MUD as well. Red represents a higher density of poles plotted, while light blue indicates a low density of poles.

Geomechanical Classification

Spacing frequency distributions for the Boone and Everton Formations show that the Boone Formation has a higher frequency of spacings between 1-5 cm (Figure 10), indicating that the Boone Formation fractures are closer together than the Everton. The length of fractures at each site do not vary considerably, except for fracture lengths measured at Everton 3, and Boone 2. Most of the fractures tend to terminate into one another, rather than terminate in the middle of

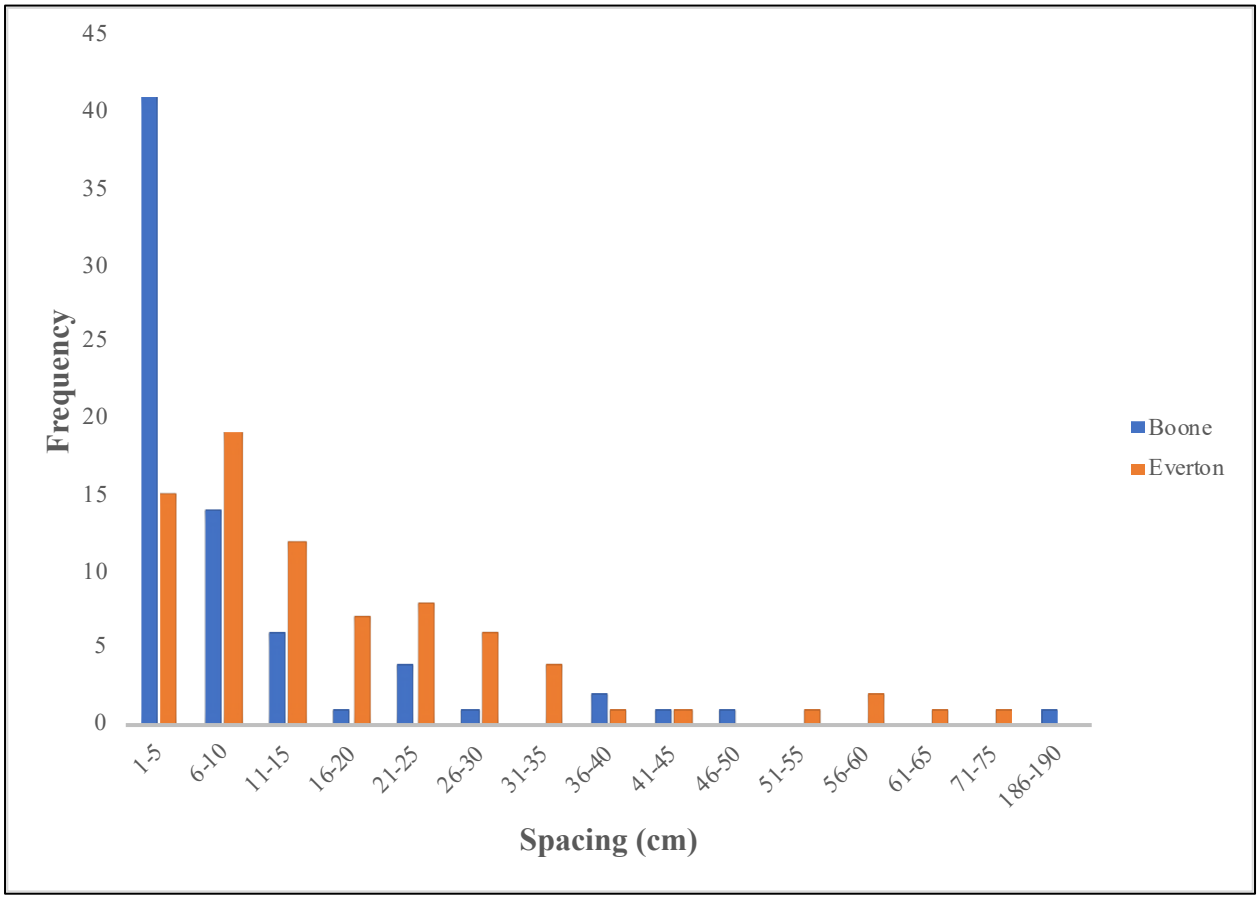

Figure 10: Spacing distributions for the Boone and Everton formations. While most of the fractures for the Boone are spaced between 1-5 cm, most for the Everton are spaced between 6-10 cm.

the rock. This style of fracture termination creates a network of blocks that can be physically weathered. The bedding planes of both formations often contribute to fracture propagation because the bedding plane is rarely flat and is often characterized by 1-5 mm of separation

between bedding contacts. Spacing, density, and length for fractures sampled at each scanline are summarized in Table 2.

Table 2: Average spacing, density, and average length for fractures measured at each scanline. The means of each of these characteristics for the Boone and Everton Formations are also listed.

Site	***Average Spacing (cm)***	***Density (fractures per meter)***	***Average Length (cm)***
Everton 1	21.8	4.4	23.2
Everton 2	10.9	8.0	16.1
Everton 3	15.4	5.7	39.2
Boone 1	17.6	5.7	14.5
Boone 2	5.23	18.6	16.3
Everton Mean	**16.0**	**6.0**	**26.2**
Boone Mean	**11.4**	**12.3**	**21.2**

Classifying different locations of the Boone and Everton Formations according to the RMR_B classification scheme shows how fractures influence overall rock strength. Both the Everton and Boone Formations have similar uniaxial compressive strengths of 73.4 MPa and 74.2 MPa, respectively. RQD values for the Everton are all higher than that of the Boone except for Everton 2, meaning that there is a larger percentage of intact rock longer than 10 cm. The groundwater conditions of the Boone are noticeably different than that of the Everton. The wetness of the fractures sampled help to further weaken the rock, along with the large separation of 1-5 mm in fractures of the Boone Formation.

RMR_B values are lower for the Boone than the Everton. These values for the Everton range from 48-67, while these values for the Boone range from 35-49. The RMR_B classification system gives a qualitative rating of a rock mass based on the final number calculated. The rock mass classified at Everton 1 is fair rock, Everton 2 is fair rock, and Everton 3 is good rock. The rock mass classified at Boone 1 is fair rock, and Boone 2 is poor rock.

Table 3: Parameters used in the calculation of the RMR_B.

Site	*UCS (Mpa)*	*RQD (%)*	*Spacing (cm)*	*Condition of Fractures*	*Groundwater (General Conditions)*	RMR_B
Everton 1	73.4	87.6	21.8	separation 1-5mm in some fractures, smooth undulating surfaces, slightly weathered walls	Completely Dry	59
Everton 2	73.4	65.7	10.9	separation 1-5mm in some fractures, weathered walls, some fractures cross bedding planes	Damp	48
Everton 3	73.4	80.6	15.4	separation < 1mm, slightly rough surfaces, slightly weathered walls	Completely Dry	67
Boone 1	74.2	86.1	17.6	separation 1-5mm in some fractures, highly weathered walls, some fractures cross bedding planes	Wet	49
Boone 2	74.2	33.3	5.3	smooth stepped surfaces, separation 1-5mm in some fractures, highly weathered walls, long continuous fractures	Damp	35

Discussion

The mean orientations of fracture sets are relatively similar for the Boone and Everton Formations, although the dominant set for each formation has a different orientation. Fracture characteristics such as length, density, and especially spacing vary between the Boone and Everton Formations. Inputting the fracture characteristics and rock mass parameters into the RMR_B scheme synthesizes the data into a complete classification of the quality and strength of the formations.

Orientation Data

Identifying fractures and other discontinuities using LiDAR scans has several advantages over traditional field mapping. Safety risks are reduced since the researcher does not need to access the rock face directly, laser surveys can be carried out rapidly, and they are often more precise (Slob et al., 2005). While these advantages make the ideal scanning location considerably easier than field methods to survey, the method is not without its disadvantages. Correctly identifying fractures using LiDAR scans relies on subtle differences in the morphology of the exposed rock face. This is contingent upon the fact that fractured zones generally have differences in relief with respect to the background rock face. In cases where fractured rock does not have a distinctly different relief than the background rock face, fractures can be difficult to identify.

Due to the nature of the valley morphology of the BNR, this issue came up when conducting investigations using Split-FX. The exposed sections of the Boone and Everton Formations at Roark Bluff and White Bluff have a relatively flat morphology in many areas, making fracture identification difficult. Also, many of the fractures present on the outcrops of each formation display as 2D fracture traces, rather than a 3D plane. Split-FX has a semi-automatic fracture extraction feature that identifies fractures based on a 3D mesh created from the LiDAR point cloud. This feature has been used to great success when analyzing highly fractured natural rock faces and roadcuts, but for this study the program often identified flat areas of the rock face as fractures (Slob et al., 2005; Kemeny et al., 2008). Although the semi-automatic fracture identification feature did not perform well during this study, fractures were still able to be identified as “fracture traces” by hand using other tools in Split-FX. Considering the problems encountered during fracture identification, the importance of field work that can

ground truth the LiDAR measurements became apparent, and in this application, solely relying on LiDAR measurements would be ill advised.

Orientation of fractures and other discontinuities affect the style of erosion in several different ways. Chiefly, the orientation plays a role in whether plucking or abrasion is the dominant erosional process in a fluvial setting. Coleman et al. (2003) determined that vertical entrainment of blocks created by near vertical fractures contributes to erosion in bedrock rivers. In the BNR, Set 2 is the dominant fracture set. It has a mean dip of 76.4 and often strikes perpendicular to the flow of the river. This creates an ideal situation by which the blocks formed by the fracture network could be plucked. The number of fracture sets also has an influence on the style of erosion. Formations with only one or two fracture sets will be more stable than systems with three or four. Including bedding planes, both the Boone and Everton formations have a higher chance of erosion by plucking mechanisms rather than abrasion because of their high set count (Scott and Wohl, 2019).

Fracture Characteristics

Whipple (2000) found that one of the chief controls on the efficacy of mechanical fluvial erosional processes is fracture spacing. Widely spaced fractures produce blocks of a size that are hard to transport (Scott and Wohl, 2019). Spacing is also the dominant characteristic that controls lateral channel widening. In the BNR, the Boone formation has a lower average spacing than the Everton Formation. Within the Boone Formation itself, fracture spacing varies depending on the dominant lithology of a given section. The massive chert beds common throughout the Boone Formation are highly brecciated and the fractures are often only 1-3 cm apart with high connectivity due to their short length. These form a fracture network in the chert

beds of the Boone that create small cuboidal blocks. Chert is a large component of the current bedload for the BNR, especially in areas downstream of the Boone Formation reaches (Keen-Zebert et al., 2017). The fact that chert is highly present in the bedload indicates that the fracture networks of the chert beds make them highly susceptible to plucking. Also, the chert in the Boone Formation was observed to be quite friable, as pieces could be picked off the wall by the researcher during field surveying.

In comparison, in areas of the Boone Formation where the chert beds are not present and the dominant lithology is limestone, the fracture spacings are similar to or even farther apart than the Everton Formation. This is evidenced by the average spacings shown for the scanline surveys at Boone 1, Everton 2, and Everton 3 in Table 2. The survey at Boone 1 contained small chert lenses that were highly brecciated but did not contain the characteristic massive chert beds. One possible explanation for the similarity in spacing between the two formations in this case is that the high solubility of the limestone in the Boone creates a scenario by which chemical weathering is preferential to mechanical weathering. Figures 11 and 12 show scanlines at Boone 2, where the chert beds were surveyed, and at Everton 2.

Figure 11: Highly brecciated chert beds surveyed at Boone 2. These fractures form a network of very small cuboidal blocks. Notice the long red fracture to the right of the researcher. Long, persistent fractures such as this are common in the chert beds of the Boone at this location. For reference, researcher is ~ 6 ft. tall.

Figure 12: Fractures surveyed at Everton 2. Fractures at locations of Roark Bluff often do not cross bedding planes. Here the bedding plane is gently dipping and can be seen to have a somewhat wide aperture, which is one of the main reasons the bedding plane is considered to contribute to instability in many areas.

Length is another characteristic that helps to set entrainment thresholds especially for block sliding and rotating. Specifically, the ratio of block height to width is important (Scott and Wohl, 2019). Findings in the BNRW for fracture length are similar between Boone 2, Everton 2, and Boone 1. Fractures are longer on average at Everton 1 and at Everton 3. This difference is partly because in these areas, the bedding plane was sampled as a discontinuity, and included in analysis. Removing bedding plane length here results in average fracture lengths that are quite similar across survey sites. Although average fracture length is similar between formations, some fractures at Boone 2 were measured at over 75 -100 cm long. None of the other locations had fractures that were persistent in this way.

Fracture density is a primary characteristic affecting erosion rates across different scales. Generally, rock erodibility scales with fracture density. Fracture density for the Boone Formation is higher than for the Everton on average, but it is especially high at Boone 2. Wohl (2008) found that whenever rocks are fractured at a submeter scale, plucking is the dominant erosional process. This density would make plucking likely along areas of the BNR where the chert beds are present, contributing to the wide valleys of the Boone Formation reaches.

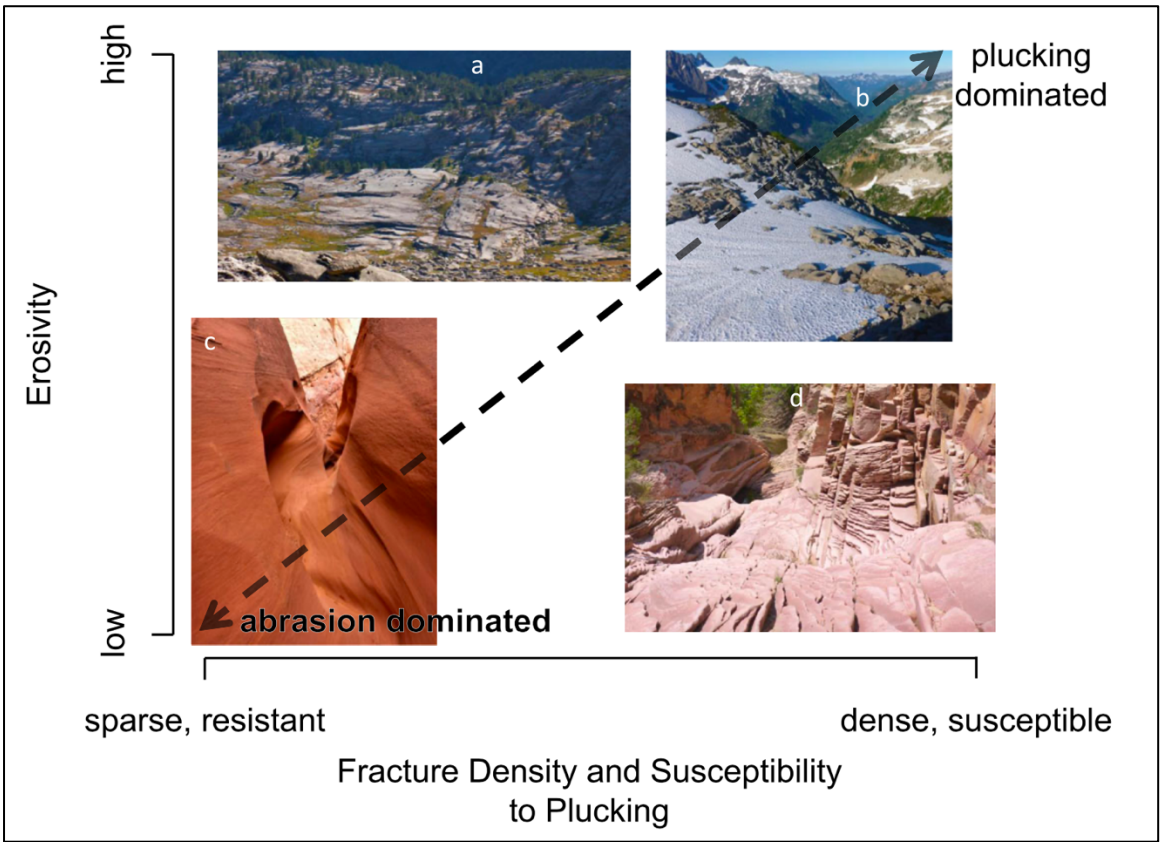

Figure 13: Conceptual diagram showing the relationship between erosivity and fracture density and susceptibility to plucking. Highly dense fractures make rock susceptible to plucking mechanisms, and less dense fractures generally create a more resistant rock that is primarily eroded by abrasion rather than plucking. Fracture density in the Boone formation suggest plucking dominance; From Scott and Wohl (2019).

The RMR_B was used to synthesize most fracture characteristics with other data about rock strength in order to see how the style of fracturing weakened the lithology. The Boone and Everton formations have very similar compressive strengths at 74.3 and 74.2 MPa, respectively.

Considering this, some other process is at work to determine valley width in the BNR than just rock strength alone. The spacing, groundwater conditions, RQD, and condition of fractures were all low for the scanline at Boone 2 compared to all other survey sites. Combining all parameters that define the style of fracturing in this area definitively shows how the chert beds of the Boone are highly susceptible to erosion. The RMR_B shows how the style of fracturing for the Boone would be a primary control on valley morphology in the BNR.

Conclusions

This study utilized remote sensing and field techniques to collect data about fracture characteristics in the BNR that were then synthesized into a geomechanical classification scheme. The study can be used to elucidate how the style of fractures and other discontinuities influence erosional susceptibility between heterogeneous lithologies exposed at river level in a setting with low tectonic activity. In the fluvial domain, fracture characteristics such as length, orientation, and especially spacing and density determine the style in which rock erodes. The style of fracturing in formations exposed along the BNR suggests plucking dominance over abrasion in both the Boone and Everton Formations. Given the similar UCS of the Boone and Everton, the final results of the geomechanical classification scheme shows how the heavily brecciated chert beds of the Boone formation served to weaken its overall strength. Erosion is localized to areas where fractures are preferentially oriented with close spacing in the Boone. This creates a scenario by which reaches composed dominantly of the Boone Formation will have wider channels and valleys than Everton Formation reaches.

Although this study developed a reach-scale rule for how the style of fracturing in heterogeneous lithologies influence erosional processes for bedrock rivers in areas of low tectonic activity, it leaves room for additional processes to be explored. It is not yet known how

vegetation present at outcrops along the BNR impedes or facilitates erosional processes. Also, how the orientation of fracture sets with respect to water flow direction affects erosion could be further explored.

Works Cited

Andriani, G.F., and Walsh, N., 2007, Rocky coast geomorphology and erosional processes: A case study along the Murgia coastline South of Bari, Apulia — SE Italy: Geomorphology, v. 87, p. 224–238, doi:10.1016/j.geomorph.2006.03.033.

Bieniawski, Z.T., 1989, Engineering rock mass classifications: a complete manual for engineers and geologists in mining, civil, and petroleum engineering: New York, Wiley, 251 p.

Braden, A., Ausbrooks, S., Mayfield, W., and Clark, J., 2003, Geologic Map of the Snowball Quadrangle, Searcy County, Arkansas: USGS Topographic, http://buffalorivergeoscience.org/maps (accessed October 2019).

Bursztyn, N., Pederson, J.L., Tressler, C., Mackley, R.D., and Mitchell, K.J., 2015, Rock strength along a fluvial transect of the Colorado Plateau – quantifying a fundamental control on geomorphology: Earth and Planetary Science Letters, v. 429, p. 90–100, doi:10.1016/j.epsl.2015.07.042.

Choi, S.Y., and Park, H.D., 2004, Variation of rock quality designation (RQD) with scanline orientation and length: a case study in Korea: International Journal of Rock Mechanics and Mining Sciences, v. 41, p. 207–221, doi:10.1016/S1365-1609(03)00091-1.

Coleman, S.E., Melville, B.W., and Gore, L., 2003, Fluvial Entrainment of Protruding Fractured Rock: Journal of Hydraulic Engineering, v. 129, p. 872–884, doi:10.1061/(ASCE)0733-9429(2003)129:11(872).

Deere, D.U., and Deere, D.W., 1989, Rock Quality Designation (RQD) After 20 Years, 102 p.

DiBiase, R.A., Rossi, M.W., and Neely, A.B., 2018, Fracture density and grain size controls on the relief structure of bedrock landscapes: Geology, v. 46, p. 399–402, doi:10.1130/G40006.1.

G. K. Gilbert, 1877, Report on the Geology of the Henry Mountains, *in* US Governement Printing Office, Washington, D.C., p. 160.

Hancock, G., Anderson, R., and Whipple, K., 1998, Beyond Power: Bedrock River Incision Process and Form, *in* Tinkler, K. and Wohl, E. eds., Rivers Over Rock: Fluvial Processes in Bedrock Channels, Washington, DC, American Geophysical Union, Geophysical monograph 107, p. 133–151, doi:10.1029/GM107p0035.

Heidner, N., 2019, Testing erosion potential of heterogeneous lithologies to understand atypical valley morphology in the Buffalo National River Watershed, Arkansas: Auburn University, 56 p., https://etd.auburn.edu/handle/10415/6629 (accessed October 2019).

Hudson, M.R., and Murray, K.E., 2003, Geologic Map of the Ponca Quadrangle, Newton, Boone, and Carroll Counties. Arkansas: USGS Topographic, https://pubs.usgs.gov/mf/2003/mf-2412/.

Katz, O., Reches, Z., and Roegiers, J.-C., 2000, Evaluation of mechanical rock properties using a Schmidt Hammer: International Journal of Rock Mechanics and Mining Sciences, v. 37, p. 723–728, doi:10.1016/S1365-1609(00)00004-6.

Keen-Zebert, A., Hudson, M.R., Shepherd, S.L., and Thaler, E.A., 2017, The effect of lithology on valley width, terrace distribution, and bedload provenance in a tectonically stable

catchment with flat-lying stratigraphy: Earth Surface Processes and Landforms, v. 42, p. 1573–1587, doi:10.1002/esp.4116.

Kemeny, J., Norton, B., Handy, J., and Donovan, J., 2008, Three-Dimensional digital imaging for the identification, evaluation, and management of unstable highway slopes: No. Highway Idea Project 119.

Keyes, C.R., 1901, Composite genesis of the Arkansas Valley through the Ozark Highlands: The Journal of Geology, v. 9, p. 486–490.

Kuniansky, E.L., 2011, U.S. Geological Survey Karst Interest Group Proceedings, Fayetteville, Arkansas, April 26-29, 2011: U.S. Geological Survey Scientific Investigations Report USGS Numbered Series 2011–5031, 218 p., http://pubs.er.usgs.gov/publication/sir20115031 (accessed October 2019).

Loye, A., Pedrazzini, A., Theule, J.I., Jaboyedoff, M., Liébault, F., and Metzger, R., 2012, Influence of bedrock structures on the spatial pattern of erosional landforms in small alpine catchments: Earth Surface Processes and Landforms, v. 37, p. 1407–1423, doi:10.1002/esp.3285.

Mcknight, E.T., 1935, Zinc and Lead Deposits of Northern Arkansas: US Geological Survey Bulletin 853.

Priest, S.D., 1993, Discontinuity Analysis for Rock Engineering: Dordrecht, Springer Netherlands, doi:10.1007/978-94-011-1498-1.

Purdue, A.H., 1901, Physiography of the Boston Mountains, Arkansas: The Journal of Geology, v. 9, p. 694–701.

Scott, D.N., and Wohl, E.E., 2019, Bedrock fracture influences on geomorphic process and form across process domains and scales: Earth Surface Processes and Landforms, v. 44, p. 27–45, doi:10.1002/esp.4473.

Slob, S., van Knapen, B., Hack, R., Turner, K., and Kemeny, J., 2005, Method for automated discontinuity analysis of rock slopes with three-dimensional laser scanning: Transportation Research Record: Journal of the Transportation Research Board, v. 1913, p. 187–194, doi:10.1177/0361198105191300118.

Smith, K.L., 2004, Buffalo River Handbook: Little Rock, Ozark Society Foundation, 436 p.

Turner, A., Kemeny, J., Slob, S., and Hack, Henri, 2006, Evaluation and management of unstable rock slopes by 3D laser scanning.

Vollmer, F.K., 1990, An application of eigenvalue methods to structural domain analysis: Geological Society of America Bulletin, v. 102, p. 786–791.

Vollmer, F.W., 1995, C program for automatic contouring of spherical orientation data using a modified Kamb method: Computers & Geosciences, v. 21, p. 31–49, doi:10.1016/0098-3004(94)00058-3.

Vollmer, F.K., 2015, Orient 3: a new integrated software program for orientation data analysis, kinematic analysis, spherical projections, and Schmidt plots: Geological Society of America Abstracts with Programs, v. 47, p. 49.

Whipple, K., 2000, River incision into bedrock: Mechanics and relative efficacy of plucking, abrasion, and cavitation: Bulletin of the Geological Society of America, v. 112, p. 490–503.

Wohl, E., 2008, The effect of bedrock jointing on the formation of straths in the Cache la Poudre River drainage, Colorado Front Range: Journal of Geophysical Research, v. 113, p. F01007, doi:10.1029/2007JF000817.

APPENDIX A:

Field Data

Table A1: Data collected in the field for the scanline at Everton 1. Projection used for location data is UTM 15N. Termination is a measurement of how fractures terminate. The designation "A" indicates a fracture that terminates at another fracture, and "I" indicates a fracture that terminates in intact rock. Fracture 24 is missing the length below, so it was not included in any fracture size calculations.

Everton 1									
Lat.	36.004574˚	Long.	-93.373056˚	Length (m)	9 m	Date	1/5/21		
Disc #	Distance (cm)	Spacing (cm)	Strike˚	Dip˚	DD˚	Length Above (cm)	Length Below (cm)	Termination	Length Above and Below (cm)
1	38	~	15	68	285	19	24	A	43
2	50	12	56	85	326	10	11	A	21
3	82	32	6	42	96	10	5	A	15
4	85	3	10	64	100	12	6	A	18
5	96	11	70	85	340	9	5	A	14
6	134	38	60	82	330	7	3	A	10
7	190	56	24	28	114	51	27	A	78
8	223	33	28	15	118	41	1	A	42
9	228	5	32	82	122	4	12	A	16
10	231	3	15	34	105	1	22	A	23
11	282	51	64	84	334	6	10	A	16
12	295	13	30	66	300	5	7	A	12
13	320	25	26	14	116	25	43	A	68
14	344	24	46	82	136	15	12	A	27
15	345	1	28	17	118	1	14	A	15
16	357	12	56	75	146	40	19	A	59
17	385	28	24	8	114	15	1	A	16
18	386	1	58	68	148	3	4	A	7
19	402	16	40	26	130	8	7	A	15
20	410	8	6	78	276	3	2	A	5
21	416	6	54	20	144	5	6	A	11

22	425	9	44	38	134	3	7	A	10
23	440	15	10	48	100	2	16	A	18
24	462	22	355	61	85	16	~	I	~
25	490	28	16	86	286	12	12	A	24
26	550	60	10	33	280	9	19	A	28
27	580	30	53	71	143	8	7	A	15
28	625	45	19	34	109	4	10	A	14
29	634	9	33	70	303	5	10	A	15
30	644	10	59	78	149	5	13	I	18
31	654	10	20	78	110	1	23	I	24
32	728	74	340	24	250	12	10	I	22
33	789	61	56	84	326	18	23	A	41
34	804	15	322	66	232	11	26	A	37
35	820	16	1	64	91	15	27	A	42
36	851	31	20	82	110	6	9	I	15
37	860	9	4	38	274	1	15	A	16
38	881	21	355	68	265	1	13	A	14
39	888	7	3	46	93	1	1	A	2
40	890	2	359	42	269	5	12	A	17

Table A2: Data collected in the field for the scanline at Everton 2.

Everton 2									
Lat.	36.040976˚	Long.	-93.337284˚	Length (m)	3	Date	1/6/21		
Disc. #	Distance (cm)	Spacing (cm)	Strike˚	Dip˚	DD˚	Length Above (cm)	Length Below (cm)	Termination	Length Above and Below (cm)
1	29	~	64	74	334	10	6	A	16
2	37	8	61	74	151	10	5	A	15
3	38	1	68	64	338	10	5	A	15
4	54	16	60	68	330	11	4	A	15
5	68	14	67	85	157	11	3	A	14
6	76	8	80	84	170	7	2	A	9
7	78	2	71	61	341	10	3	A	13
8	85	7	76	55	346	5	5	A	10
9	105	20	78	44	348	9	10	A	19
10	126	21	75	65	345	7	11	A	18
11	159	33	88	64	358	3	11	I	14
12	171	12	75	70	345	8	12	A	20
13	174	3	68	66	338	8	14	A	22
14	184	10	70	66	340	10	5	A	15
15	195	11	65	67	155	10	3	A	13
16	205	10	105	78	195	4	6	I	10
17	207	2	58	68	328	6	1	A	7
18	224	17	65	78	155	2	~	I	~
19	229	5	76	76	346	10	14	A	24
20	238	9	74	71	164	5	10	A	15
21	245	7	100	84	190	13	3	A	16
22	264	19	95	72	5	15	6	A	21
23	278	14	35	88	305	13	10	A	23

24	280	2	96	73	6	13	14	A	27

Table A3: Data collected in the field for the scanline at Everton 3.

Everton 3									
Lat.	36.043661˚	Long.	-93.341206˚	Length	3	Date	1/6/21		
Disc. #	Distance (cm)	Spacing (cm)	Strike˚	Dip˚	DD˚	Length Above (cm)	Length below (cm)	Termination	Length Above and Below (cm)
1	19	~	60	86	330	14	15	I	29
2	30	11	300	78	30	15	10	A	25
3	57	27	308	76	38	15	20	A	35
4	80	23	305	85	35	15	13	A	28
5	105	25	68	85	338	15	50	A	65
6	107	2	34	71	304	13	1	A	14
7	137	30	32	89	302	15	46	A	61
8	161	24	30	78	300	15	16	A	31
9	162	1	40	54	130	1	40	A	41
10	190	28	28	80	298	15	30	A	45
11	191	1	33	45	123	1	15	A	16
12	210	19	30	82	300	13	20	A	33
13	220	10	26	80	296	15	30	I	45
14	235	15	28	88	298	15	50	I	65
15	245	10	350	81	260	15	20	A	35
16	255	10	25	65	295	20	3	A	23
17	265	10	60	66	330	25	50	I	75

Table A4: Data collected in the field for Boone 1. This scanline started at 210 cm on the measuring tape due to field conditions. All spacing values were recalculated using the first fracture as a starting point. Due to this, the first fracture has a distance of 0.

Boone 1										
Lat.	35.974084˚	Long.	-92.890535˚	Length	6.1	Date	1/7/21			
Disc #	Distance (cm)	True Dist. (cm)	Spacing (cm)	Strike˚	Dip˚	DD˚	Length Above (cm)	Length Below (cm)	Termination	Length Above and Below (cm)
1	210	0	~	53	74	143	30	45	I	75
2	255	45	45	45	70	315	2	15	A	17
3	257	47	2	80	76	350	2	2	A	4
4	260	50	3	83	64	353	2	3	A	5
5	266	56	6	73	88	343	2	3	A	5
6	270	60	4	73	88	343	2	3	A	5
7	274	64	4	73	88	343	2	3	A	5
8	284	74	10	73	88	343	2	3	A	5
9	290	80	6	73	88	343	2	3	A	5
10	293	83	3	73	88	343	2	3	A	5
11	296	86	3	73	88	343	2	3	A	5
12	300	90	4	73	88	343	2	3	A	5
13	302	92	2	73	88	343	2	3	A	5
14	307	97	5	73	88	343	2	3	A	5
15	308	98	1	75	66	345	8	5	A	13
16	345	135	37	340	71	70	15	3	A	18
17	368	158	23	54	61	324	5	15	A	20
18	405	195	37	68	86	338	60	2	A	62
19	430	220	25	48	51	318	40	1	A	41
20	445	235	15	58	68	328	30	1	A	31
21	470	260	25	24	75	294	10	2	A	12

22	498	288	28	44	90	314	6	2	A	8
23	505	295	7	20	55	290	10	3	A	13
24	516	306	11	292	73	22	13	3	A	16
25	705	495	189	43	74	313	5	3	A	8
26	720	510	15	44	81	314	1	8	A	9
27	738	528	18	45	74	135	3	5	A	8
28	785	575	47	55	57	325	3	3	A	6
29	790	580	5	30	60	300	3	5	A	8
30	795	585	5	30	60	300	3	5	A	8
31	796	586	1	30	60	300	3	5	A	8
32	800	590	4	30	60	300	3	5	A	8
33	805	595	5	30	60	300	3	5	A	8
34	808	598	3	30	60	300	3	5	A	8
35	810	600	2	70	70	340	15	30	A	45

Table A5: Data collected in the field for Boone 2.

MW 1									
Lat.	35.966160°	Long.	-92.852706°	Length	2.1	Date	1/7/21		
Disc. #	Distance (cm)	Spacing (cm)	Strike	Dip	DD	Length Above (cm)	Length Below (cm)	Termination	Length Above and Below (cm)
1	8	~	320	70	50	5	1	A	6
2	19	11	293	82	23	10	15	A	25
3	21	2	340	80	70	10	3	A	13
4	26	5	340	80	70	13	3	A	16
5	28	2	340	80	70	5	3	A	8
6	29	1	340	80	70	3	5	A	8
7	30	1	340	80	70	10	5	A	15
8	35	5	340	80	70	10	3	A	13
9	40	5	340	80	70	8	3	A	11
10	41	1	340	80	70	5	1	A	6
11	46	5	340	80	70	5	5	A	10
12	48	2	320	55	50	5	2	A	7
13	54	6	339	86	69	3	10	A	13
14	60	6	339	86	69	3	3	A	6
15	70	10	340	22	70	80	20	A	100
16	75	5	290	71	20	2	3	A	5
17	82	7	290	71	20	1	5	A	6
18	87	5	290	71	20	3	3	A	6
19	102	15	290	71	20	5	2	A	7
20	109	7	290	75	20	8	3	A	11
21	110	1	330	54	60	8	5	A	13
22	111	1	335	57	65	10	3	A	13
23	113	2	335	58	65	8	4	A	12

24	119	6	310	68	40	8	3	A	11
25	124	5	330	80	60	8	2	A	10
26	135	11	320	80	50	7	5	A	12
27	140	5	307	82	37	7	5	A	12
28	142	2	307	82	37	9	5	A	14
29	143	1	307	82	37	7	4	A	11
30	145	2	307	82	37	6	3	A	9
31	151	6	270	74	180	7	3	A	10
32	152	1	270	74	180	8	3	A	11
33	154	2	270	74	180	6	11	A	17
34	158	4	270	74	180	5	1	A	6
35	181	23	300	75	30	3	2	A	5
36	185	4	337	84	67	3	2	A	5
37	191	6	295	86	25	8	1	A	9
38	198	7	280	85	10	20	2	A	22
39	207	9	324	71	54	84	57	A	141

APPENDIX B:

LiDAR Data

Table B1: Orientation data for fracture traces identified within Split-FX for the Everton Formation. Station is the specific point cloud that the fracture was identified in.

ID	Station	Dip Direction	Dip
1	Ev1ATraces	221.9	89.5
2	Ev1ATraces	224.8	86.8
3	Ev1ATraces	49.3	88.6
4	Ev1ATraces	231.5	85.2
5	Ev1ATraces	226.7	80.8
6	Ev1ATraces	231.1	82.3
7	Ev1ATraces	224.7	74.5
8	Ev1ATraces	305.7	29.6
9	Ev1ATraces	222.2	86.2
10	Ev1ATraces	220.7	74.2
11	Ev1ATraces	78.9	36.7
12	Ev1ATraces	231.7	80.6
13	Ev1ATraces	300.6	15.2
14	Ev1ATraces	302.3	13.9
15	Ev1ATraces	316.4	3.1
16	Ev1ATraces	301.4	7.8
17	Ev1ATraces	294.6	5.1
18	Ev1ATraces	281.6	4
19	Ev1ATraces	267.8	84.5
20	Ev1ATraces	268.3	87.9
21	Ev1ATraces	294.3	8.3
22	Ev1ATraces	313.6	4.9
23	Ev1ATraces	270.2	1.5
24	Ev1ATraces	232.5	49.6
25	Ev1ATraces	286.1	13
26	Ev1ATraces	289.8	11.6
27	Ev1ATraces	79.3	86.6
28	Ev1ATraces	211.6	87.9
29	Ev1ATraces	262.9	15.6
30	Ev1ATraces	217	72
31	Ev1ATraces	217.1	38.1
32	Ev1ATraces	227.3	42.6
33	Ev1ATraces	317.6	85.3
34	Ev1ATraces	319.5	89.2
35	Ev1ATraces	198.4	5.3
36	Ev1ATraces	325.6	47.8
37	Ev1ATraces	281.2	18.2
38	Ev1ATraces	306.1	14.6
39	Ev1ATraces	308	87.8

40	Ev1ATraces	249.9	81
41	Ev1ATraces	304.9	8
42	Ev1ATraces	308.7	5
43	Ev1ATraces	305.7	16.6
44	Ev1ATraces	74.7	88.1
45	Ev1ATraces	258.7	88.4
46	Ev1ATraces	63	89.8
47	Ev1ATraces	252.3	77
48	Ev1ATraces	271.7	6.5
49	Ev1ATraces	308.7	14.5
50	Ev1ATraces	313.9	25.4
51	Ev1ATraces	353.4	0.4
52	Ev1ATraces	220.7	62.7
53	Ev1ATraces	245.5	79.3
54	Ev1ATraces	320.6	15.2
55	Ev1ATraces	304.1	9.8
56	Ev1ATraces	312.9	25.1
57	Ev1ATraces	292.3	4.7
58	Ev1ATraces	289.5	14.7
59	Ev1ATraces	188	3.1
60	Ev1ATraces	75.5	68.7
61	Ev1ATraces	307.9	18.2
62	Ev1ATraces	231.3	86.9
63	Ev1ATraces	49.3	87.3
64	Ev1ATraces	45.1	88.5
65	Ev1ATraces	259.7	74
66	Ev1ATraces	200.9	59.5
67	EV1BTraces	268.6	62.1
68	EV1BTraces	282.8	1
69	EV1BTraces	261.4	61
70	EV1BTraces	118.1	6
71	EV1BTraces	342	5.1
72	EV1BTraces	265.5	54.9
73	EV1BTraces	209	67.5
74	EV1BTraces	321.4	18.8
75	EV1BTraces	317.5	19.3
76	EV1BTraces	50.7	88.4
77	EV1BTraces	257.9	89.8
78	EV1BTraces	61.4	82.7
79	EV1BTraces	262	47.8
80	EV1BTraces	262.2	59.5
81	EV1BTraces	249.9	72.1
82	EV1BTraces	286.2	76.8
83	EV1BTraces	269.1	65.9
84	EV1BTraces	31.3	9.1

85	EV1BTraces	294.7	28.3
86	EV1BTraces	323.9	47.7
87	EV1BTraces	286	2.8
88	EV1BTraces	267.6	58.3
89	EV1BTraces	252	82.6
90	EV1BTraces	76	88.4
91	EV1BTraces	65.4	77.5
92	EV1BTraces	70.3	77.6
93	EV1BTraces	67	86.7
94	Ev2ATraces	36.3	86.9
95	Ev2ATraces	10.3	81.4
96	Ev2ATraces	328.6	17.7
97	Ev2ATraces	12.5	15.3
98	Ev2ATraces	225.5	88.2
99	Ev2ATraces	218.8	87.5
100	Ev2ATraces	37.7	50.7
101	Ev2ATraces	85.8	88.6
102	Ev2ATraces	71.8	82.4
103	Ev2ATraces	38.9	88.4
104	Ev2ATraces	37	80.1
105	Ev2ATraces	50.9	77.8
106	Ev2ATraces	141.5	9.6
107	Ev2ATraces	217.3	89.2
108	Ev2ATraces	50.4	89.8
109	Ev2ATraces	344.4	10.6
110	Ev2ATraces	226.8	85.2
111	Ev2ATraces	227.1	80.8
112	Ev2ATraces	49.1	87.7
113	Ev2ATraces	51.4	80.5
114	Ev2ATraces	162.5	26.5
115	Ev2ATraces	239.3	84.7
116	Ev2ATraces	352.8	8.2
117	Ev2ATraces	28.4	87
118	Ev2ATraces	31.9	61.1
119	Ev2ATraces	323.9	13.6
120	Ev2ATraces	312	14.7
121	Ev2ATraces	262.2	63
122	Ev2ATraces	20.7	86.5
123	Ev2ATraces	45.8	75.9
124	Ev2ATraces	356.9	35
125	Ev2ATraces	231.9	88.5
126	Ev2ATraces	22.5	11
127	Ev2ATraces	34.8	13.2
128	Ev2ATraces	76.4	9.5
129	Ev2ATraces	234.9	87.2

130	Ev2ATraces	236.9	86.3
131	Ev2ATraces	15.2	9
132	Ev2ATraces	39.1	88.9
133	Ev2ATraces	359.3	22.7
134	Ev2ATraces	0.4	25.3
135	Ev2ATraces	231.5	88.9
136	Ev2ATraces	1.8	26.7
137	Ev2ATraces	16	15.4
138	Ev2ATraces	231.4	86.2
139	Ev2ATraces	347.5	24
140	Ev2ATraces	241.2	84.3
141	Ev2ATraces	4.3	26
142	Ev2ATraces	49.5	89.7
143	Ev2ATraces	238	85.7
144	Ev2BTraces	66	67.4
145	Ev2BTraces	105.9	12
146	Ev2BTraces	276.6	84.6
147	Ev2BTraces	105.6	87.5
148	Ev2BTraces	258.4	89.2
149	Ev2BTraces	88.6	5.6
150	Ev2BTraces	339.1	1.1
151	Ev2BTraces	352.4	19.5
152	Ev2BTraces	353.7	22.2
153	Ev2BTraces	331.6	4
154	Ev2BTraces	359.8	2.8
155	Ev2BTraces	353.8	8.1
156	Ev2BTraces	42.1	78.3
157	Ev2BTraces	353.2	9.6
158	Ev2BTraces	59.8	75
159	Ev2BTraces	58.6	86
160	Ev2BTraces	35.7	67.8
161	Ev2BTraces	53.1	68.1
162	Ev2BTraces	51.3	73.1
163	Ev2BTraces	83.8	78
164	Ev2BTraces	324.8	2.1
165	Ev2BTraces	5.1	10.9
166	Ev2BTraces	44.8	81.2
167	Ev2BTraces	85.6	12.2
168	Ev2BTraces	45.6	78.8
169	Ev2BTraces	53.9	10.4
170	Ev2BTraces	235.6	88
171	Ev2BTraces	30.1	4.9
172	Ev2BTraces	25.7	7.3
173	Ev2BTraces	359.8	8.5
174	Ev2BTraces	168.5	0.7

175	Ev2BTraces	2.6	8.3
176	Ev2BTraces	73.6	68.3
177	Ev2BTraces	79.9	58.6
178	Ev2BTraces	179.4	25.3
179	Ev3ATraces	289	83.1
180	Ev3ATraces	290.8	67.1
181	Ev3ATraces	299.7	79.2
182	Ev3ATraces	302	84.3
183	Ev3ATraces	310.3	27.9
184	Ev3ATraces	270.3	44.7
185	Ev3ATraces	227.9	83.3
186	Ev3ATraces	58	83.8
187	Ev3ATraces	59	72.8
188	Ev3ATraces	81.3	61.6
189	Ev3ATraces	127.8	88.6
190	Ev3ATraces	129.2	67.3
191	Ev3ATraces	249.3	78.5
192	Ev3ATraces	285	86.2
193	Ev3ATraces	272.6	74.3
194	Ev3ATraces	264.5	53.1
195	Ev3ATraces	272.7	63.1
196	Ev3ATraces	277.3	55.4
197	Ev3ATraces	288.7	76.7
198	Ev3ATraces	58	73.8
199	Ev3ATraces	73.4	85.5
200	Ev3ATraces	330.8	40.7
201	Ev3ATraces	263.8	62.1
202	Ev3ATraces	284.1	53.2
203	Ev3ATraces	280.9	67.9
204	Ev3ATraces	302.7	71.5
205	Ev3ATraces	294.3	66.4
206	Ev3ATraces	303.3	54.8
207	Ev3ATraces	294	73.2
208	Ev3ATraces	105.4	87.6
209	Ev3ATraces	112.2	83
210	Ev3ATraces	297.6	76.1
211	Ev3ATraces	295	88.3
212	Ev3ATraces	121.5	86.8
213	Ev3ATraces	283.5	83.2
214	Ev3ATraces	95.7	86.5
215	Ev3ATraces	275.1	85.6
216	Ev3ATraces	283.9	84.5
217	Ev3ATraces	103.5	89.9
218	Ev3ATraces	114.5	74.8
219	Ev3ATraces	106.9	87

220	Ev3ATraces	131.5	85.4
221	Ev3ATraces	94.2	86.4
222	Ev3ATraces	131.3	21.8
223	Ev3ATraces	163.6	26.6
224	Ev3ATraces	130.4	90
225	Ev3ATraces	142.9	81.6
226	Ev3ATraces	143.2	82.1
227	Ev3ATraces	150.8	82.1
228	Ev3ATraces	128.5	70.8
229	Ev3ATraces	98.8	73.9
230	Ev3ATraces	279.4	87.8
231	Ev3ATraces	110.1	80.5
232	Ev3ATraces	102.1	80.3
233	Ev3ATraces	106.4	76
234	Ev3ATraces	136	79
235	Ev3ATraces	102.8	79.8
236	Ev3ATraces	133	80.9
237	Ev3ATraces	105	63.1
238	Ev3ATraces	241.1	74
239	Ev3ATraces	227.9	82.8
240	Ev3ATraces	136	81.2
241	Ev3ATraces	212.8	26.1
242	Ev3ATraces	42	82.8
243	Ev3ATraces	211.6	87
244	Ev3ATraces	66.1	82.6
245	Ev3ATraces	171.1	71
246	Ev3ATraces	153.3	63.7
247	Ev3ATraces	153.5	82.8
248	Ev3ATraces	175.8	86.1
249	Ev3ATraces	180.8	83.6
250	Ev3ATraces	9.3	88
251	Ev3ATraces	9.8	70
252	Ev3ATraces	151.3	81.7
253	Ev3ATraces	12	82.6
254	Ev3ATraces	198.1	87.5
255	Ev3ATraces	10.4	87.7
256	Ev3ATraces	173.6	6.9
257	Ev3ATraces	187.1	2.5
258	Ev3ATraces	171.2	4.2
259	Ev3ATraces	163.6	5.6
260	Ev3ATraces	191.9	14.9
261	Ev3ATraces	174.7	31.7
262	Ev3ATraces	12.3	4
263	Ev3ATraces	9.4	21.5
264	Ev3ATraces	10	22.2

265	Ev3ATraces	14.1	13.8
266	Ev3ATraces	354.6	6.7
267	Ev3ATraces	350.2	5.3
268	Ev3ATraces	8.4	15.5
269	Ev3ATraces	186	17.5
270	Ev3ATraces	174.6	6.9
271	Ev3ATraces	163.8	16.9
272	Ev3ATraces	162.8	6.9
273	Ev3ATraces	359.2	9
274	Ev3ATraces	219.1	1.2
275	Ev3ATraces	197.3	12.9
276	Ev3ATraces	94.1	2.8
277	Ev3ATraces	184.8	18.2
278	Ev3ATraces	15.1	4.7
279	Ev3ATraces	202.6	3.6
280	Ev3ATraces	339.6	2.2
281	Ev3ATraces	174.5	2
282	Ev3ATraces	346.6	4
283	Ev3ATraces	15.4	5.6
284	Ev3ATraces	185	0.8
285	Ev3ATraces	174.1	7.4
286	Ev3ATraces	282.6	67.2
287	Ev3ATraces	228.7	87.1
288	Ev3ATraces	39.7	82.8
289	Ev3ATraces	221.4	79.1
290	Ev3ATraces	110.9	85.3
291	Ev3ATraces	92.3	76.9

Table B2: Orientation data for fracture traces identified within Split-FX for the Boone Formation. Station is the specific point cloud that the fracture was identified in.

ID	Station	Dip Direction	Dip
1	BooneATrace	36.8	7
2	BooneATrace	293.5	78.3
3	BooneATrace	48.4	11.3
4	BooneATrace	96.6	84.6
5	BooneATrace	109.8	88.8
6	BooneATrace	22.9	27.4
7	BooneATrace	12.4	30.4
8	BooneATrace	178.9	8.2
9	BooneATrace	12	40.9
10	BooneATrace	20.3	29
11	BooneATrace	20.2	19.6
12	BooneATrace	16.4	17.7
13	BooneATrace	88.8	68.7
14	BooneATrace	89.6	31.4
15	BooneATrace	44.3	17.1
16	BooneATrace	91.2	73.5
17	BooneATrace	50.2	8.1
18	BooneATrace	7.6	7.6
19	BooneATrace	342.1	3.8
20	BooneATrace	183.3	26.6
21	BooneATrace	185.1	22.5
22	BooneATrace	177.5	11.5
23	BooneATrace	123	80.8
24	BooneATrace	246.5	89.8
25	BooneATrace	217.5	67.5
26	BooneATrace	158.5	10.3
27	BooneATrace	47.4	80.3
28	BooneATrace	217.5	79.9
29	BooneATrace	329.9	19.7
30	BooneATrace	31.5	3
31	BooneATrace	105.9	81.2
32	BooneATrace	19.4	10.3
33	BooneBTrace	4.9	18.1
34	BooneBTrace	344.8	14.3
35	BooneBTrace	207.9	8.2
36	BooneBTrace	305.4	29.3
37	BooneBTrace	229.3	9.3
38	BooneBTrace	320.4	27.5
39	BooneBTrace	289.8	42.7

40	BooneBTrace	325	39.6
41	BooneBTrace	34.6	47.6
42	BooneBTrace	303.3	48.5
43	BooneBTrace	320.6	38.2
44	BooneBTrace	268.9	11.6
45	BooneBTrace	37.2	8.2
46	BooneBTrace	335.9	9.5
47	BooneBTrace	342.7	42.1
48	BooneBTrace	357.8	51
49	BooneBTrace	331.9	34.5
50	BooneBTrace	311.1	18.7
51	BooneBTrace	316.4	16.5
52	BooneBTrace	353.1	16.8
53	BooneBTrace	279.7	87.4
54	BooneBTrace	279.6	77.1
55	BooneBTrace	182.1	30.2
56	BooneBTrace	199.1	14.9
57	BooneBTrace	235.1	35.3